

Project information

Project full title	European network for developing new horizons for RIs
Project acronym	EURIZON
Grant agreement no.	871072
Instrument	Research and Innovation Action (RIA)
Duration	01/02/2020 – 31/01/2024
Website	https://www.eurizon-project.eu/

Deliverable information

Deliverable no.	4.16
Deliverable title	Final technical report with detailed beam dynamics studies and documentation for EBS and/or PETRA IV
Deliverable responsible	DESY
Related Work-Package/Task	WP4 Task 1
Type (e.g. Report; other)	Report
Author(s)	S.M.Liuzzo, N.Carmignani, L.Carver, L. Hoummi, T.Perron, S.White, I. Agapov, J. Keil, L.Malina, E.Musa, B. Veglia, T.Hellert
Author(s) affiliation	ESRF, Grenoble France DESY, Hamburg, Germany
Dissemination level	Public
Document Version	1
Date	18 December 2023
Download page	

Document information

Version no.	Date	Author(s)	Comment
1	18 Dec 2023	S.M.Liuzzo, N.Carmignani, L.Carver, L. Hoummi, T.Perron, S.White, I. Agapov, J. Keil, L.Malina, E.Musa, B. Veglia, T.Hellert	
1.1	04 Jan 2024		Format complemented by J. Marauska



Table of Contents

Introduction.....	3
Task 4.1 activities	3
Magnetic cross-talks for EBS and PETRA IV	3
Studies to define an appropriate approach to include cross-talks effect in the lattice model.....	4
Higher order cross-talks	6
Effect of cross-talks in correctors magnets	6
Effect of cross-talks between quadrupole magnets.....	8
EBS simulations with detailed multipoles along dipoles.....	10
Further steps	12
MDT activities at EBS and PETRA III for storage ring optimizations.....	12
Lifetime optimizations using Extremum Seeker.....	13
Lifetime optimizations using Badger	19
Measurement and analysis of TbT data analysis to determine Storage ring optics	29
Definition of a new functions for errors and correction based on pyAT	33
Implementation of a pyAT based commissioning simulation toolkit.....	34
Correction using pyAT based commissioning simulation toolkit	36
Implementation and use of analytic formulas	38
Typical output of commissioning simulations in pyAT.....	40
Python simulated commissioning	42
Translation by ChatGPT	42
Library components.....	42
Usage examples.....	45
PySC summary and future work	49
Future plans for pyAT developments	49
Other activities related to the Task 4.1	50
AT workshop on 2-3rd October	50
Conclusions.....	53
Publications	54



Introduction

The beam dynamics studies of the work package 4.1 aim at developing tools and concepts that can be used for the next generation light sources. The outcome of the discussions during Milestone meetings M4.1.1, M4.1.2 and M4.1.3 has been the definition of the following specific list of activities:

1. Study the impact of magnetic cross-talks among neighboring magnets in the H7BA lattice of EBS and H6BA lattice of PETRA IV.
2. Machine Dedicated Time (MDT) experimental activities at EBS and PETRA III for Storage Ring (SR) optimizations:
 - a. Using available optimizers, among which Extremum Seeker¹ and Badger²+XOpt³
 - b. Measurement and analysis of Turn-by-Turn (TbT) data analysis to determine storage ring optics
3. Definition of new functions for errors and correction based on pyAT for commissioning simulations of new storage ring projects.

The activities listed above are detailed in the following sections.

In point 1 and 3 existing numerical tools based on the Accelerator Toolbox will be adapted and extended to be used by EBS, PETRA IV and potentially any other storage ring light source. The algorithms, software, techniques and procedures developed could be used during the design and commissioning phases of future storage ring projects or to enhance the performance of existing machines.

The study of magnetic cross-talks (in 1) and measurement of optics with TbT data (in 2b) improve lattice modeling strategies. Point 2a explicitly performs online lattice optimization and correction. Point 3 simulates realistic operation conditions including errors and correction sequences.

The developed tools in all points have been applied to the ESRF-EBS and the PETRA IV lattice models. The injection efficiency and the lifetime of both storage rings have been optimized with success during several successful machine dedicated times at the ESRF and DESY.

Task 4.1 activities

Magnetic cross-talks for EBS and PETRA IV

To improve storage ring (SR) lattice modeling, magnetic cross talks between neighboring magnets should be included in the lattice files at an early stage, before commissioning of the storage ring. We call cross-talk the magnetic field modifications observed when two magnets (either electromagnets or

¹ A. Scheinker, “Model independent beam tuning”, IPAC 2013, TUPWA068

² Zhang, Zhe, and USDOE. Badger: The Ocelot Optimizer Rebirth. Computer software. <https://www.osti.gov/servlets/purl/1874964>. USDOE. 4 Aug. 2021. Web. doi:10.11578/dc.20220706.3.

³ R. Roussel, C. Mayes, A. Edelen, A. Bartnik, Xopt: A simplified framework for optimization of accelerator problems using advanced algorithms, *JACoW IPAC2023 (2023) THPL164*, [10.18429/JACoW-IPAC2023-THPL164](https://doi.org/10.18429/JACoW-IPAC2023-THPL164)



permanent magnets) are at a very short distance (order of the magnets gaps or bore radius, ~50mm for fourth generation light sources) one with respect to the other.

For the EBS storage ring only dipolar cross-talk effects were considered initially and no action was taken in terms of lattice modeling. Later, once the SR commissioning started a large tune discrepancy (~1.3 units in the vertical plane) was observed. This discrepancy was solved by introducing quadrupolar cross-talk effect in the lattice^{4,5}. Introducing such an effect in the model earlier would have spared approximately 15 days of commissioning time for EBS; more had this effect not been spotted immediately. For future SR light sources such as PETRA IV it is then mandatory to include such effects before commissioning.

In the framework of this project we address cross-talk effects in several ways: 1) studies to define an appropriate approach to include cross-talk effects in the lattice model, making use of a minimum number of elements and allowing optics matching; 2) higher order cross-talks, in particular sextupolar cross-talks; 3) effect of cross-talks in corrector magnets and quadrupole magnets for PETRA IV, 4) high-order multipoles longitudinal distribution.

Studies to define an appropriate approach to include cross-talks effect in the lattice model

Dipole cross-talks are not to be included in lattice modeling. Their effect has to be considered at the magnet design stage, for example as was done for the EBS lattice, increasing the field of dipole magnets modules close to quadrupoles. When installed the dipole field becomes the nominal one and the quadrupole magnetic center will be measured.

Quadrupole cross-talks are computed by Radia simulation¹³ and have to be introduced in the SR lattice.

The simplest solution is a static-hard-edge model represented by additional fixed field multipoles placed at the correct locations. An example of such a model is visible in Figure 1. Quadrupolar cross-talks represented in Figure 1 have two effects: one is the generation of some negative quadrupole gradient at the edge of the neighboring dipole, the other is a reduction of the gradient of the quadrupole itself (the field leaked to the dipole). The first effect is modeled in a static-hard-edge model as a thin lens at the side of the dipole. The second effect is a correction factor that must be computed and considered for magnet calibration.

⁴ <https://link.aps.org/doi/10.1103/PhysRevAccelBeams.24.072401>

⁵ <https://link.aps.org/doi/10.1103/PhysRevAccelBeams.24.110701>



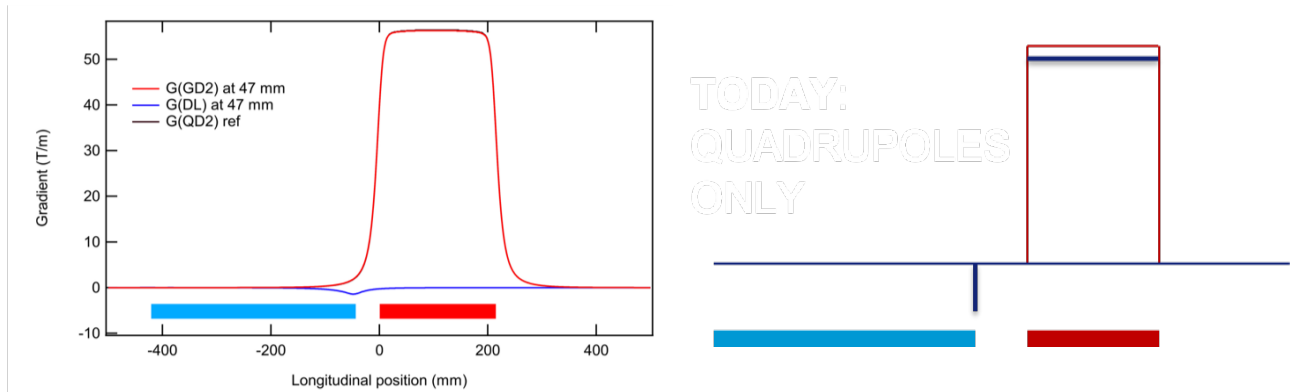


Figure 1: Left: quadrupole-dipole cross-talks; Right: static-hard-edge model. The red curves are the field of the quadrupole as if it was far from the dipole. The blue lines represent schematically the field changes to be modeled when the magnets are at their design distance of 47 mm.

The additional lenses (18 for the EBS lattice cell, 22 for the injection cell) included in the lattice model imply optics changes that must be compensated by an adequate redefinition of the quadrupole magnets strengths. This process is called optics matching.

With a static-hard-edge model the additional thin lenses do not change their value during the optics matching.

A first step to improve the optics model would be to link the main magnet quadrupole gradients to their corresponding cross-talk effects. When the gradients of the main quadrupoles are varied, so are the cross-talk lenses. This may be easily done in codes such as MAD8 and MADX. It is less trivial to be done in more modern codes, such as AT⁶ and pyAT⁷, due to the way in which matching scripts are defined. A solution proposed towards a dynamic-hard-edge model is a redefinition of the lattice models to a format similar to MAD8⁸, MADX⁹, elegant¹⁰, SAD¹¹, OPA¹² and others.

An example is given below:

⁶ 10.18429/JACoW-IPAC2015-MOPWA014

⁷ <https://atcollab.github.io/at/p/index.html>

⁸ https://cern.ch/mad8/doc/phys_guide.pdf

⁹ <https://www.google.com/search?client=firefox-b-d&q=MADX+guide>

¹⁰ https://ops.aps.anl.gov/manuals/elegant_latest/elegant.html

¹¹ <https://acc-physics.kek.jp/SAD/>

¹² <https://ados.web.psi.ch/opa/>



```
function ring = S28_Longitudinal(Dip,Kquads,Ksext,Koct)

% element definitions
% ...

qf1_1= atmultipole('QF1',5e-3,'PolynomB',{1,2},Kquads(1)*0.01,'PolynomB',{1,1},Kdip(1)*0.01);
qf1_2= atmultipole('QF1',5e-3,'PolynomB',{1,2},Kquads(1)*0.2,'PolynomB',{1,1},Kdip(1)*0.01);
qf1_3= atmultipole('QF1',5e-3,'PolynomB',{1,2},Kquads(1)*0.5,'PolynomB',{1,1},Kdip(1)*0.01);
qf1_4= atmultipole('QF1',5e-3,'PolynomB',{1,2},Kquads(1)*0.7,'PolynomB',{1,1},Kdip(1)*0.01);
qf1_5= atmultipole('QF1',5e-3,'PolynomB',{1,2},Kquads(1)*0.9,'PolynomB',{1,1},Kdip(1)*0.01);
qf1_6= atmultipole('QF1',5e-3,'PolynomB',{1,2},Kquads(1)      , 'PolynomB',{1,1},Kdip(1)*0.01);

QF1h = [qf1_1,qf1_2,qf1_3,qf1_4,qf1_5,qf1_6,qf1_6,qf1_6,qf1_6,qf1_6];
QF1 = [QF1h;QF1h(end:-1:1)];

% ...

% build lattice out of blocks
ring = [QF1, Drift, DL, SF2...
]

end
```

This solution, although familiar to the accelerator community and intuitive, is not easily implemented in AT, due to the available matching techniques.

AT matching scripts that make use of the thin lenses already available in the model are under investigation and will be assessed during the project.

Presently the process of implementation of quadrupolar cross-talks in the PETRA IV lattice model is stale, awaiting data from the magnet design.

Since no better modeling has been selected yet, the EBS lattice model has also not been updated and still relies on a static-hard-edge model implementation.

Higher order cross-talks

Cross-talks concern multipoles of all orders installed in the SR. In the EBS optics sextupoles and octupoles are present. Due to an observed discrepancy among the measured and model chromaticity (about 1% in both planes), the introduction of sextupole cross-talk effects may give at least a partial answer to this issue.

The modelization of sextupole cross-talks in the EBS and PETRA IV models is awaiting for RADIA magnetic model data and could not progress during the Eurizon Task 4.1.

Effect of cross-talks in correctors magnets

The design of the magnets for PETRA IV is still ongoing and not all magnet designs exist at the moment. The design work is concentrating on the most demanding magnets which are the quadrupoles of the triplet near the undulators (QD0, QF1, QD2) with large gradients up to 115 T/m and the combined-function magnets (DLQ). The combined-function magnets have a longitudinal gradient and are made of permanent magnets. Magnetic field simulations of the three quadrupoles in the triplet are the most advanced and optimized designs exist based on OPERA-3D calculations.

As a first example of the effect of cross-talk between magnets in the PETRA IV lattice the assembly of two quadrupoles QF1 (type PQB) and QD2 (type PQC) and a fast corrector magnet (FC) has been calculated and data were provided by the magnet design group of DESY. The corrector magnet will be installed with equal distance of 79 mm to the yokes of nearby quadrupoles (Figure 2).



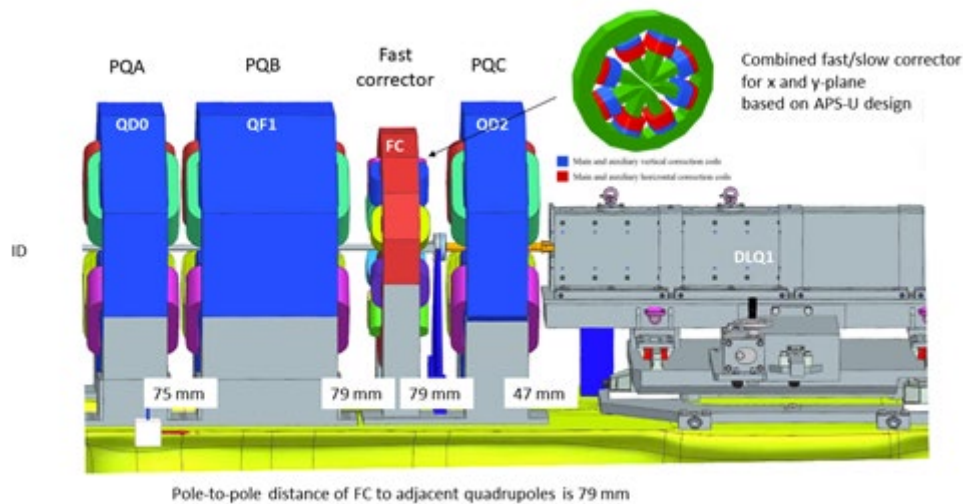


Figure 2: Assembly of a fast corrector (FC) between two quadrupoles (QF1 and QD2) used for cross talk simulations in the quadrupole triplet of PETRA IV. The triplet consists of the three quadrupoles PQA (QD0), PQB (QF1) and PQC (QD2).

The corrector magnet has an octupole-like magnet yoke and is based on a design which was developed for APS-U. The corrector magnet combines fast and slow coils for orbit correction in the horizontal and vertical plane and has a better field quality compared to conventional designs using dipole magnets.

The multipole expansion of the B-field as a function of the longitudinal position for five different cases was provided: the two quadrupoles and the corrector alone without any other magnets nearby, the assembly of the three magnets with only the quadrupoles powered and the assembly of the three magnets with all magnets powered. Only the effect of the horizontal slow corrector magnet was simulated and nominal currents were assumed.

The cross-talk reduces the vertical field component of the corrector magnet in the fringe field region and leads to a reduction of the field integral of ~4%. The largest effect occurs near the edges of the nearby yokes of the quadrupoles (Figure 3, blue curve, black arrows).

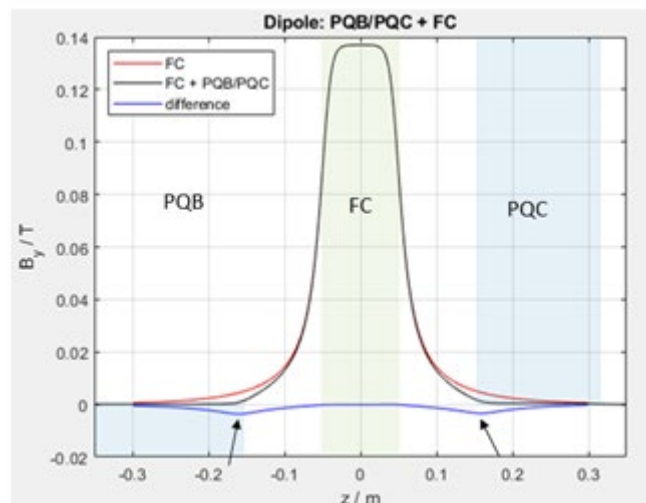


Figure 3: Change of the vertical field component of the corrector without (red) and with the quadrupoles (black). The field difference is shown in blue. Blue and green areas are the hard edge models for the quadrupoles and corrector magnets.

A simple model to take the cross-talk of the corrector magnet into account would be the use of a hard-edge model with a corrected calibration curve and two zero-length correctors with negative dipole field integrals at the edges of the quadrupoles.

The change of the quadrupole gradients due to the excitation of the fast corrector is shown in Fig. 4. It can be seen that the cross-talk reduces mainly the gradient of PQC (nearly 1%) while the gradient of the PQB quadrupole is mostly unaffected. Different saturation of the quadrupoles could be the reason for this. In addition, changes of the gradient appear near the edges of the yokes of the quadrupoles and the corrector.

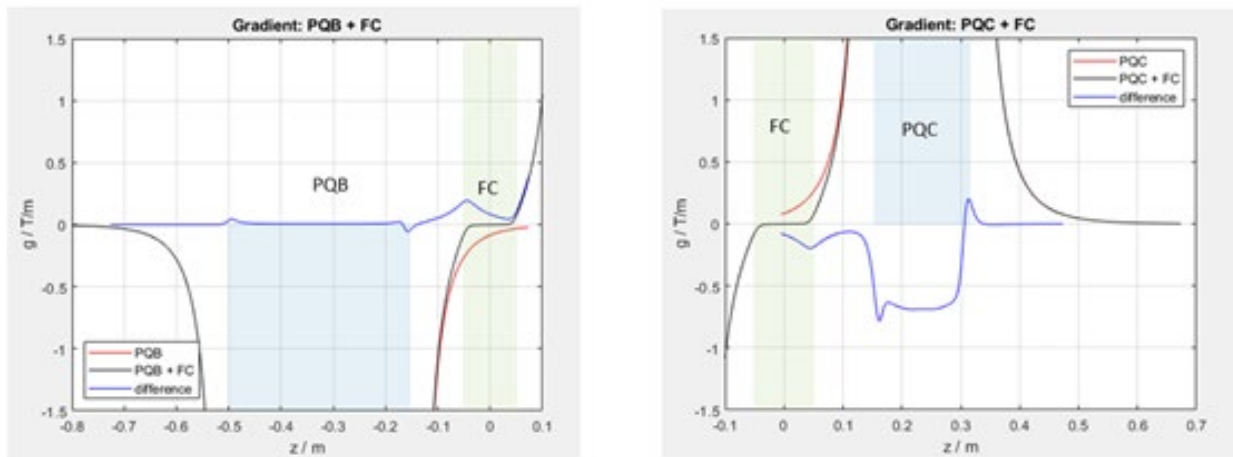


Figure 4: Change of the gradients of the quadrupoles without (red) and with the fast corrector (black). The difference of the gradient is shown in blue. Left picture for PQB, right picture for PQC. Blue and green areas are the hard edge models for the quadrupoles and the corrector magnet.

For the two quadrupoles, the effect of the cross-talk could be modeled by using a hard-edge field approximation of the quadrupoles with a corrected calibration curve and several zero-length quadrupoles with negative integrated gradients at the edges of the quadrupoles and the corrector.

These simple models – although not perfect – would already be useful to take cross-talks into account and would help to improve the lattice model of PETRA IV. A better agreement could be achieved by using the measured longitudinal distribution as it was described in the previous section.

Effect of cross-talks between quadrupole magnets

As a second example, the cross-talk between the two quadrupoles PQA (QD0) and PQB (QF1) in the quadrupole triplet of PETRA IV has been computed with OPERA-3D. The positions of these quadrupole magnets in the H6BA cell of PETRA IV is shown in Fig. 2. The calculation was done by the magnet design group at DESY.

Three different cases were analyzed: The quadrupoles PQA alone, the quadrupole PQB alone, and the assembly of both quadrupoles. The longitudinal field profiles of the PQA alone (red), PQB alone (red),

and the assembly of a PQA and PQB (black) are shown in Fig. 5. The field difference between the gradient profile of a single quadrupole and the assembly of both quadrupoles is shown in blue (multiplied by a factor of 10).

Both quadrupoles have a bore radius of 22 mm and the distance between yokes is only 75 mm. For such a small distance, crosstalk is not negligible and changes in gradients will occur. The reduction of the gradients in the body of PQA and PQB are 0.8 T/m and -2.0 T/m. The integrated gradients change by 1.0% for the PQA and 1.8% for the PQB because of the cross-talk between the magnets.

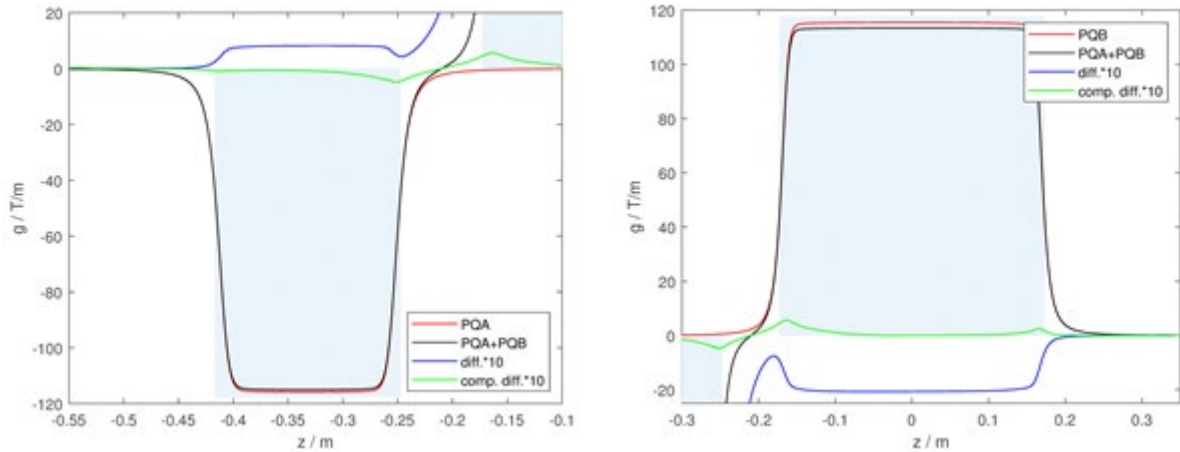


Figure 5: Change of the longitudinal gradient profile due to cross talk between PQA (left picture) and PQB (right picture). The profile for a single PQA or PQB is shown in red, the profile for the assembly of PQA and PQB is shown in black. The blue line is the difference (multiplied by a factor of 10). The green curve is the profile difference (multiplied by a factor of 10) after correction of the gradient reduction. Blue areas are the hard edge models for the quadrupoles.

Such large changes of the gradients would produce unacceptable optics distortions without correction. As all quadrupoles will have individual power supplies it is possible to compensate for the reduced integrated gradients by increasing the quadrupole currents of the power supplies accordingly. However, even after compensating the gradient reduction for the assembly of PQA-PQB by taking the gradient reduction into account (green curve) there remains some local uncompensated gradient errors. These errors appear mainly near the edge of the yokes of PQA and PQB.

The change of the optical functions in the H6BA cell of PETRA IV due to cross-talk was computed with a simplified model by taking the gradient errors into account. The quadrupole strengths were reduced according to the integrated gradient reduction from magnet simulation of the assembly of the quadrupoles. The gradient errors near the edges were simulated by adding thin quadrupole lenses at these locations. With both sources of gradient errors, the effect on the optical functions would be a change of ~22% of the beta function in the horizontal plane and a change of ~30% in the vertical plane. The simulation shows that by increasing the integrated gradients of PQA (QD0), PQB (QF1) and PQC (QD2) the optics distortion can be almost fully corrected (Fig. 6).

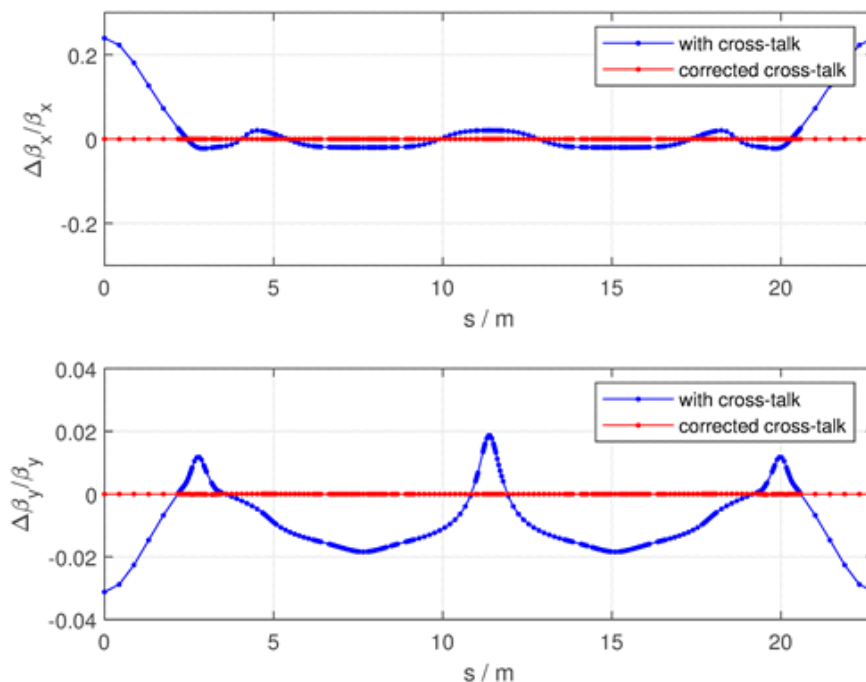


Figure 6: Beta-beating due to cross-talk (blue) and after correction of the cross-talk effect (red) in the quadrupole triplets the H6BA cell of PETRA IV.

More details about the simulation of cross-talk and the influence of the optical functions in the PETRA IV H6BA triplet can be found in a recent publication¹³.

No further data concerning cross talks was provided by the ESRF and DESY magnet design group.

EBS simulations with detailed multipoles along dipoles

For the EBS lattice multipoles up to the 20th order were computed by J.Chavanne (ESRF Insertion device and magnets group) along a Longitudinal gradient Dipole (DL) magnet composed of 5 modules. The integral of each component is corrected to zero both in simulations and after measurement for the real magnets. However, the pattern along the DL (that is about 1.7m long) could lead to some modification in the nonlinear optics due to the variation of beta functions along the magnet. The following figure represents the simulated multipoles in a DL magnet. Similar data is available for the DQ magnets.

¹³ J. Keil, I. Agapov, A. Aloev, R. Bartolini and M. Thede,, "Cross-talk between magnets in the H6BA-cell of PETRA IV", presented at the IPAC'23, Venice, Italy, May 2023, paper WEPM032, unpublished.



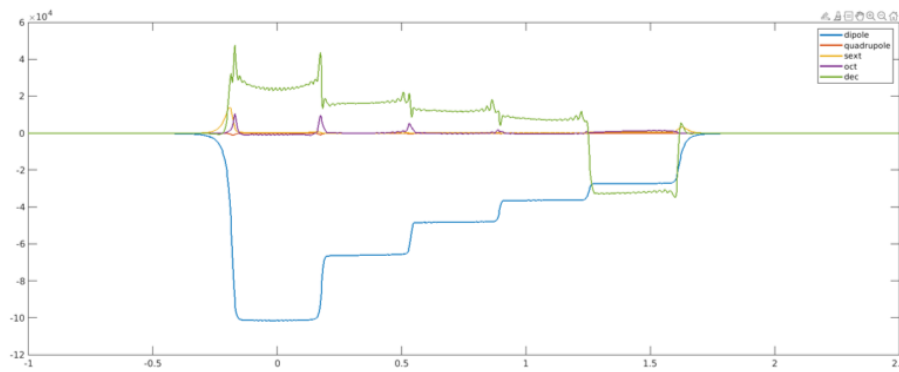


Figure 7: Multipoles from dipole to decapole along a DL1 EBS longitudinal gradient dipole. Arbitrary units scaled for visibility.

In particular for the EBS there is a known discrepancy between measured and simulated: 1) dispersion, 2) chromaticity, 3) vertical detuning with horizontal amplitude. A different dipole field distribution along the beam trajectory could explain the difference in dispersion. An additional sextupole component could contribute to chromaticity. All other multipoles could account for vertical detuning with amplitude. It is thus of interest to see the effect of such multipoles on the lattice optics.

These multipole components are known with a precision of 1 mm. The lattice is then sliced in 1 cm elements (1 mm slicing generates lattices too large for practical use) and the longitudinal multipoles are added to each slice in the lattice. The resulting optics are depicted in the figures below.

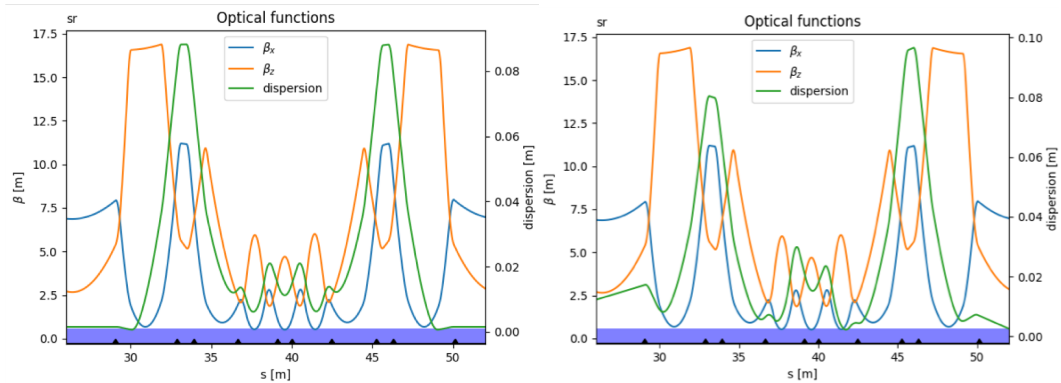
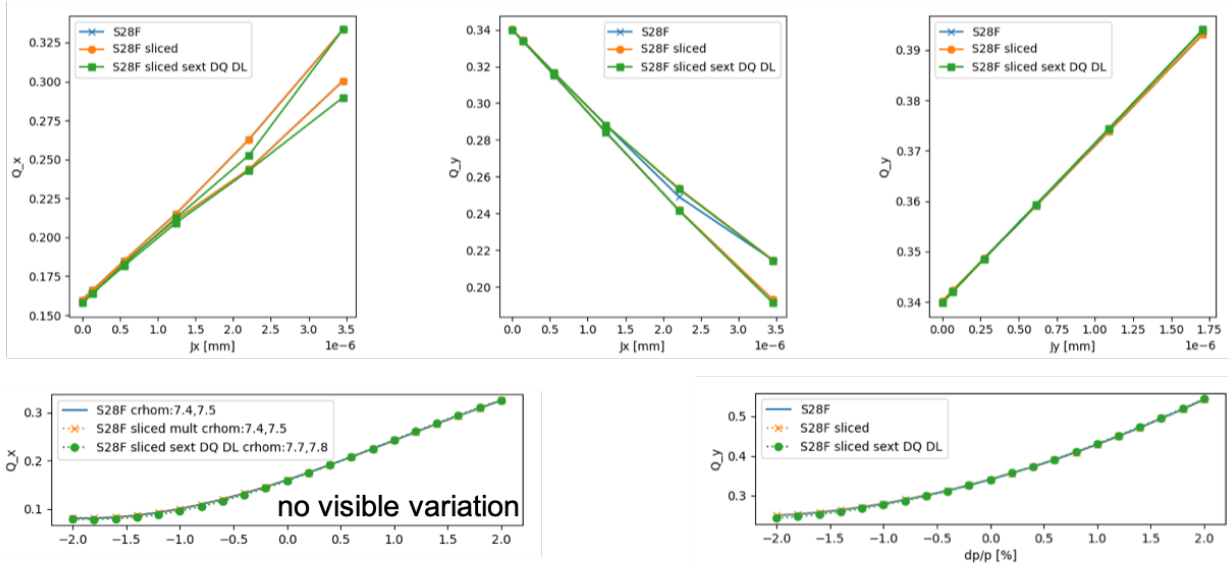


Figure 8: Left: Sliced optics model without longitudinal multipoles. Right: Sliced optics model with longitudinal multipoles.

In the figure on the right, including the additional multipoles, the dispersion is not periodic any more, as expected due to the additional fields.

These lattices are then used for computation of detuning with amplitude and momentum (chromaticity). Despite the visible changes in optics, there is no visible effect on the detuning with amplitudes and momentum (see Figure 8-bis), thus the multipoles included in the simulations are not sufficient to explain the discrepancy among EBS measurements and simulations.



(10^4 m^{-1})	$dv_x/dQ_x, dv_y/dQ_y$	dv_x/dJ_x	dv_y/dJ_x	dv_y/dJ_y
Measurement	$(9.6 \pm 0.5, 9.2 \pm 0.5)$	4.7 ± 0.2	-10.9 ± 0.3	19 ± 2 Indirect, no vertical kicker
Simulation	$(7.4, 7.1)$	4.35	-4.20	$+3.13$

Figure 8-bis: Top: horizontal tune vs horizontal amplitude, vertical tune vs horizontal amplitude, vertical tune vs vertical amplitude. Middle line: horizontal and vertical tune vs energy deviation. Bottom line: table of measured vs expected values.

These results will be presented at the IPAC2024 conference.

Further steps

The work done above concerning cross-talks will also benefit any other lattice upgrade that foresees installing magnets very close to each other. The application of common schemes to two different light sources, forces the development to be as general as possible, thus leading to more versatile solutions that may be adopted also by other existing or planned SR. The lack of data from magnetic simulations reduced the extent of the studies, but nevertheless allowed to further investigate alternative options as a fully sliced model, that resulted to be unrealistic for use in operation and did not give explanation for the discrepancies among model and measurement for the EBS lattice.

MDT activities at EBS and PETRA III for storage ring optimizations

Common MDT activities were planned at the EBS and PETRA III storage ring to target optimization and determination of machine parameters. The measurement and optimization techniques used are adapted from existing ones and point to develop and enforce the use of sharable tools among several facilities.

Machine Dedicated Time (MDT) for experimental activities at EBS and PETRA III has been allocated for several studies:

- Lifetime and vertical emittance optimizations using Extremum Seeker¹⁴ and Badger+XOpt,

¹⁴ A. Scheinker, "Model independent beam tuning", IPAC 2013, TUPWA068



- Injection efficiency optimization at EBS and PETRA III,
- Measurement and analysis of TbT data analysis to determine storage ring optics.

Lifetime optimizations using Extremum Seeker

Summarized description of the optimizer

The Extremum Seeker (ES) is a local, model-independent algorithm¹⁵. It requires a cost function which may be analytically unknown $\hat{C}(p, t)$, but which depends on accelerator parameter settings and must be maximized or minimized. The algorithm adjusts the parameters p_j according to:

$$\frac{dp_j}{dt} = \sqrt{\alpha\omega_j} \cos[\omega_j t + k\hat{C}(p, t)]$$

Where $\alpha > 0$ is the dithering amplitude, the frequencies $\omega_j = \omega r_j$ and $r_j \neq r_i$ for $i \neq j$. The term $k > 0$ is the feedback gain. In case of maximization k is chosen negative.

Implementation begins by setting parameter values to some initial conditions, $\mathbf{p}(1)$, recording the cost function $C(1)$, and then performing the update:

$$p_j(2) = p_j(1) + \Delta\sqrt{\alpha\omega_j} \cos[\omega_j\Delta + k\hat{C}(p, t)]$$

with $\Delta = 2\pi/(10 * \max\{\omega_j\})$ being the discrete time step small enough so that the finite difference approximation of ES dynamics is accurate with the highest frequency component requiring at least 10 steps to complete one full oscillation. The algorithm was adapted from the existing version implemented in the Ocelot simulation toolkit¹⁶.

ES, with its ability to handle open-loop unstable, time-varying, nonlinear systems, is an ideal candidate for online persistent control and optimization of complex, many parameter, large systems. Because the dynamic feedback for stabilization and optimization is model-independent, can tune multiple parameters simultaneously and is robust to measurement noise, it has gained popularity in particle accelerator applications, since accelerators are usually very large complex systems with many magnet components and time-varying beam distributions. This method has been applied to accelerators around the world including adaptive online model tuning for non-invasive electron beam diagnostics at the Facility for Advanced Accelerator Experimental Tests (FACET) at SLAC National Accelerator Laboratory¹⁷.

¹⁵ A. Scheinker and M. Krstić, "Minimum-Seeking for CLFs: Universal Semiglobally Stabilizing Feedback Under Unknown Control Directions," in *IEEE Transactions on Automatic Control*, vol. 58, no. 5, pp. 1107-1122, May 2013, doi: 10.1109/TAC.2012.2225514.

¹⁶ https://github.com/ocelot-collab/optimizer/tree/master/op_methods

¹⁷ Scheinker, Alexander, and Spencer Gessner. "Adaptive method for electron bunch profile prediction." in *Physical Review Special Topics-Accelerators and Beams* 18.10 (2015): 102801. <https://doi.org/10.1103/PhysRevSTAB.18.102801>



Work done to prepare the MDT

The algorithm was first tested on a simple cost function (plotted below in Figure 9) varying the hyperparameters (k_{ES} and α) to understand their impact on the optimization routine.

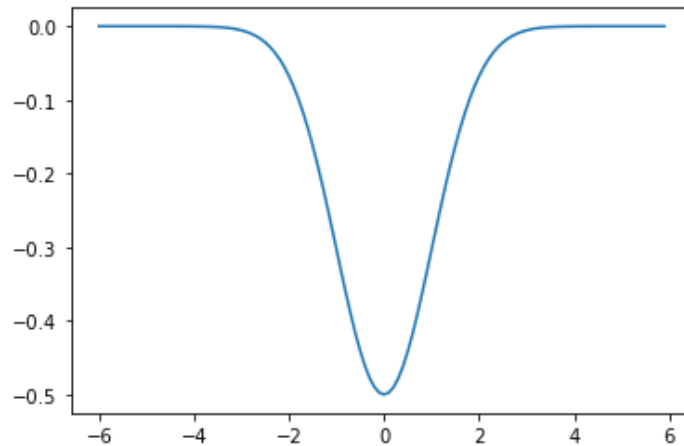


Figure 9: Simple example of the cost function used to test the ES algorithm code.

Increasing the value of k_{ES} leads the routine to converge towards the minimization of the simple cost function chosen as example (see Figure 10).

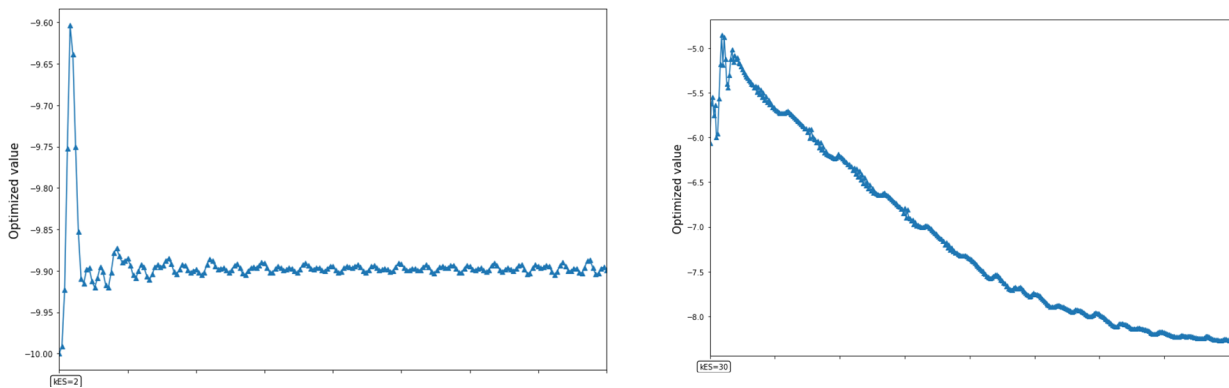


Figure 10: Evolution of the example cost function during the minimization routine with two different values of $k_{ES}=2$ (left) and $k_{ES}=30$ (right).

Successively the ES optimizer was tested in pyAT¹⁸ simulations for the EBS storage. The chosen target of the simulated optimization is minimum vertical emittance. Two cases were addressed. In the first case the vertical emittance was increased intentionally setting a random value for the skew quadrupole strength of a single skew quadrupole (on an SF2 sextupole). In the second case, all skew quadrupoles were set to random values. The ES algorithm was used in both cases to minimize the vertical emittance

¹⁸ <https://atcollab.github.io/at/p/index.html>



calculated by the pyAT program. The variables used for the minimization were 32 skew quadrupole strengths of the SF2A family.

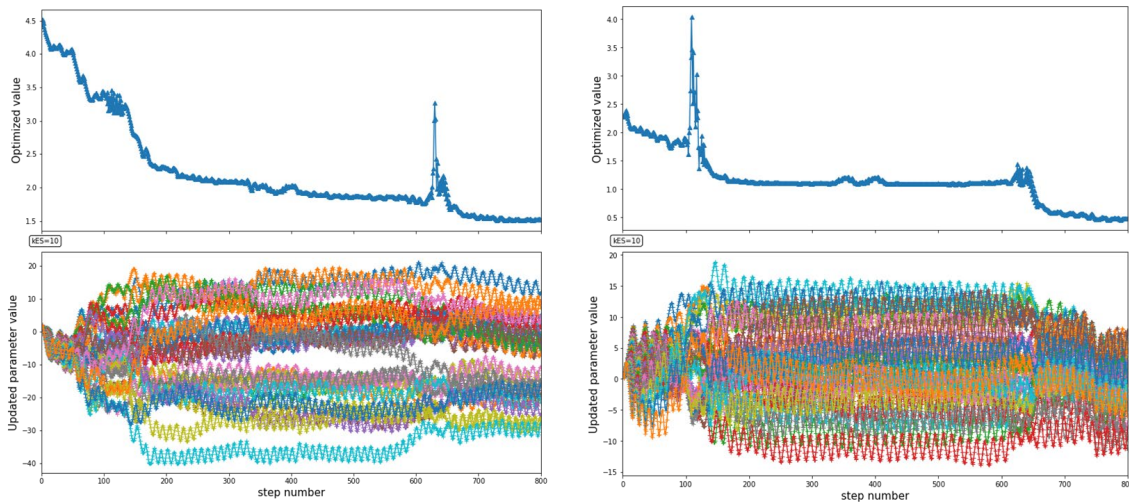


Figure 11: Left: only one skew quad of the SF2A in the pyAT simulated lattice is used to induce an increase on the vertical emittance (optimized value, top) which is minimized by the ES algorithm tuning 32 SF2A knobs (updated parameter value, bottom). Right: all the skew quads are used and compensated with the same knobs as the left figure.

In the first case ES was expected to find exactly the value of the single magnet moved. In the second case there was no particular expectation on the pattern of corrections. Figure 11 shows the result of these 2 simulated optimizations scenarios. In both cases the ES optimizer finds an improved solution for the vertical emittance.

Other tests in preparation of the MDT were performed also using the EBS control system simulator¹⁹. Several features were added to the ES algorithm to improve its user-friendliness:

- Updated figures which plots the evolution of the minimized value(s) and the sent amplitudes contained in the vector x with the number of iterations (e.g. Fig. 11),
- A data saving function in python which includes the correction strengths of the skew quadrupoles for testing in the ESRF-EBS storage ring.

Description of the MDT activity

Following the promising simulations, the ES algorithm was tested on the ESRF-EBS storage ring during a four-hour machine dedicated time (MDT) on November 28th 2022. As proof of principle and to work on a low-current beam, the ES was adapted to the vertical emittance minimisation tested in simulation rather than lifetime optimizations (the final target of these studies). The waiting time, added to ensure the skew quadrupoles arrive at the requested strengths and that the read value of the vertical emittance has stabilized, is set to 5 seconds.

The plan of the MDT was as follows:

1. Vertical emittance minimisation: first test

¹⁹ S.Liuzzo et al. "The EBS simulator: a commissioning booster" [10.18429/JACoW-ICALEPCS2021-MOPV012](https://doi.org/10.18429/JACoW-ICALEPCS2021-MOPV012)



1. Detune **ONE SF** skew quadrupole
 2. Save SRMagnet file
 3. Scan the parameters
 4. Try the ES algorithm with 32 SF skew including the detuned one.
 5. Save the SR Magnet file
 6. Compare the vertical emittance before and after
2. If satisfactory,
1. Send random errors in the skew quadrupoles
 2. Save SR Magnet file
 3. Scan the parameters
 4. Try the ES algorithm with 32 SF skew.
 5. Save the SR Magnet file
 6. Compare the vertical emittance before and after

The ESRF-EBS electron beam has a low equilibrium vertical emittance of 0.5 ± 0.1 pm.rad. The Extremum Seeking algorithm was run through a Jupyter notebook in the ESRF-EBS control room. The MDT started with the introduction of a $+0.005$ m⁻¹ correction strength in **one skew**, located at a sextupole of the SF2A family (see Fig. 12), which increases the vertical emittance to 3.9 ± 0.1 pm.rad. The minimisation will be conducted using all the 32 skew quadrupoles located at the SF2A sextupoles.

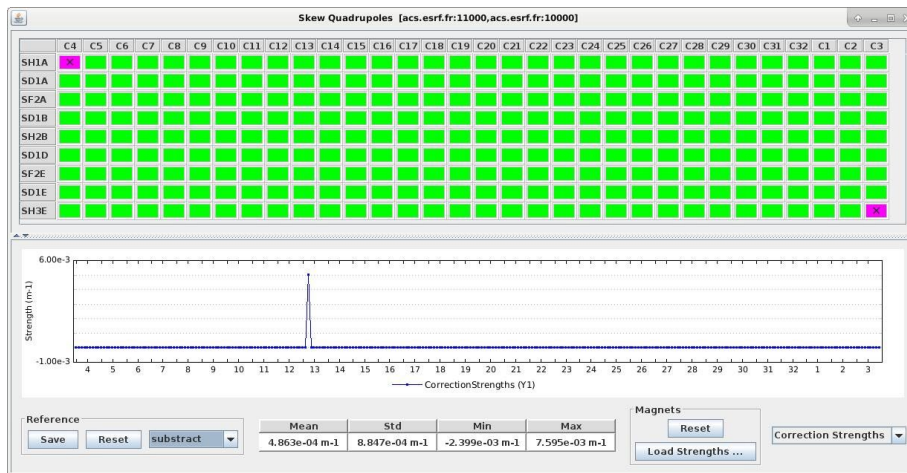


Figure 12: Skew quadrupole correction strengths at the beginning of the MDT. The application shows the difference between the current strengths and the nominal strengths.

The first minimisation is launched with the standard hyperparameters $\alpha = 3 * \alpha_0$ and $k_{ES} = 40$ which provided a good response in simulations. The result of the first 70 iterations as well as the sent amplitudes are displayed in Fig. 13 left. Two limitations are spotted: the amplitudes reach too large values, and the first observed reduction from 3.9 to 2.9 pm.rad is not aggressive enough to ensure a fast minimisation. Therefore, the boundaries were decreased from $[-8;8]$ to $[-5;5]$, and k_{ES} decreased to 30 to limit the impact of the read emittance value in the perturbation function. The results are displayed in Fig. 13 right. The conducted changes are followed by small variations in the vertical emittance around the starting point. This minimisation was stopped when the emittance blew up with increased amplitudes of the skew quadrupole strengths. The first step was not successful: first, the very localized error on one skew, although simple to correct, still triggers a global response of the selected knobs. Then, it appears the ES algorithm loses knowledge of the previous found minimum and



struggles to go back. The time constraints of the MDT as well as the duration of each ES run forced us to move on with the tests.

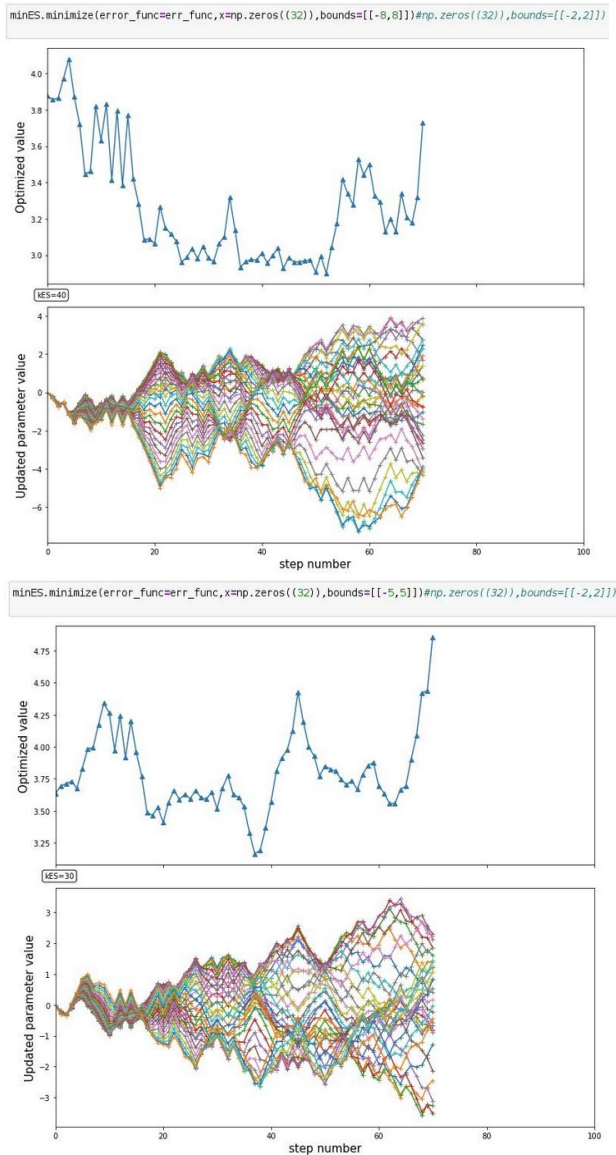


Figure 13: Evolution of the vertical emittance (top figures) and amplitudes sent to the skew quadrupoles on the SF2A during two Extremum Seeking sessions (left) with $\alpha = 3 \cdot \alpha_0$, bounds = [-8:8] and $k_{ES} = 40$ and (right) $\alpha = 3 \cdot \alpha_0$, bounds = [-5:5] and $k_{ES} = 30$.

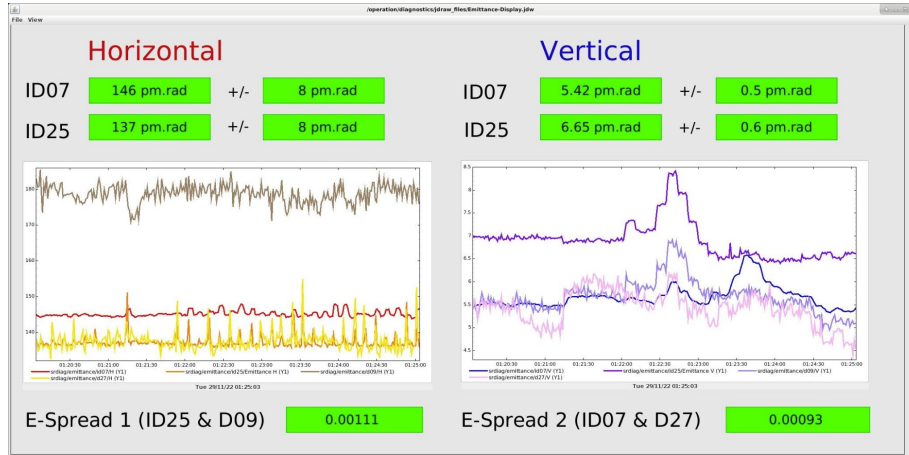


Figure 14: Emittance measurements in the ESRF-EBS storage ring during the first iterations of an ES minimisation of parameters $\alpha = 6 \cdot \alpha_0$, bounds = [-5;5] and $k_{ES} = 30$. The emittances are calculated at two pinholes in the SR. The reference is measured in ID07, which corresponds to the red and blue lines for the horizontal and vertical emittances respectively.

Instead of perturbing one skew, we sent random errors to all skew quadrupole, limited to 1% strength change, which generated a vertical emittance of 5.7 pm.rad. The next ES run used the same hyperparameters as the latest run, and the same knobs. The variation in vertical emittance were of the 10^{-3} order, so the parameter α was increased to $6 \cdot \alpha_0$. Figure 14 illustrates the variation of the emittances at the beginning of this minimisation.

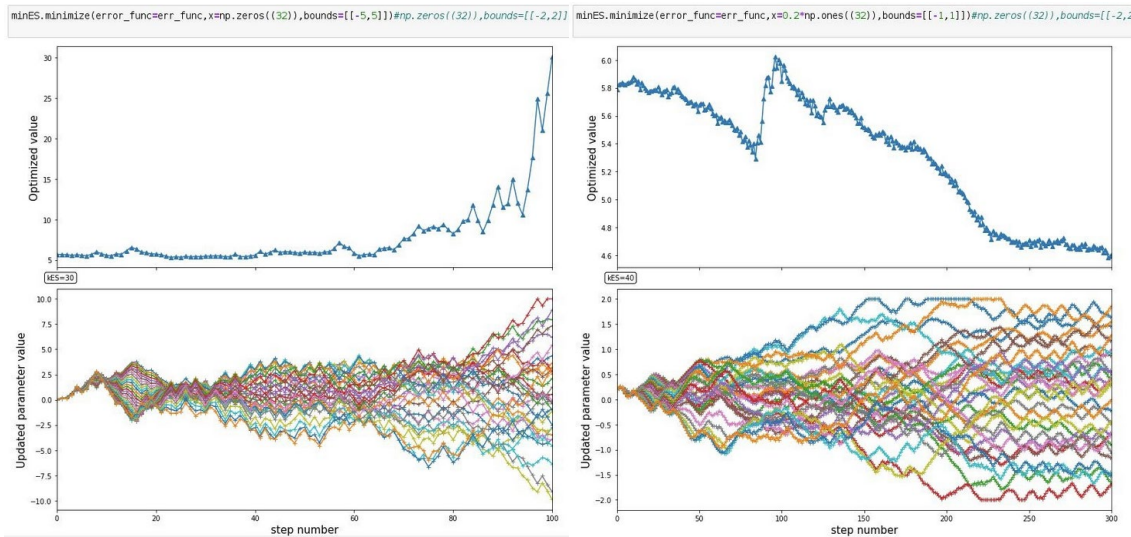


Figure 15: Left: ES minimisation of parameters $\alpha = 6 \cdot \alpha_0$, bounds = [-5;5] and $k_{ES} = 30$. Right: ES minimisation of parameters $\alpha = 2 \cdot \alpha_0$, bounds = [-1;1] and $k_{ES} = 40$.

Despite presenting small and promising variations in the vertical emittance, this minimisation ended with large amplitudes in the skew quadrupoles exceeding the input boundaries, and a blow up of the emittance from 5 pm.rad to about 30 pm.rad, as seen in Fig. 15, left. This phenomenon is to be avoided in a future version of the algorithm, with for instance a control on the maximum emittance allowed with a restoration to a previous minimum. A last test drastically reduced the boundaries on the amplitudes to [-1;1] and increased k_{ES} to 40 to start a minimisation sooner, and reduced $\alpha = 2 \cdot \alpha_0$ to slow down the amplitude variations. The previous skew quadrupole corrections are replaced with new



small (less than 1% variation) random strengths, for a vertical emittance of 5.8 pm.rad. The evolution of the amplitudes and vertical emittance during this minimisation is in Fig. 15, right. The boundaries were respected and triggered a stronger minimisation after the 200 step. The minimisation ended after reaching its maximum iteration number which resulted in a total emittance reduction of 1.2 pm.rad.

The vertical emittance minimisation study of the ES algorithm on the ESRF-EBS storage ring had limited results. Firstly, a long time is required to select the hyperparameters of the ES, and a simple scan is not efficient. Future simulations should aim at reducing the time allocated for the hyperparameter selection. Secondly, a 20% reduction of the emittance was achieved after 30 minutes, with no convergence of the algorithm. To make the algorithm more robust and avoid stagnation to local minimum, an evaluation of the convergence during the minimisation could be implemented. This additional module would estimate a possible local minimum and modify the hyper-parameter α to increase the amplitude of the perturbation and scan a larger scale, and increase k_{ES} to increase the impact of the cost function on the parameter update. This could speed up the convergence and make the ES a more time-efficient algorithm. Provided further simulations dedicated to lifetime optimisation, a future MDT could be planned using an improved version of Extremum Seeking algorithm or different tools, such as Badger²⁰. It would then be compared to the current lifetime optimisation conducted on the ESRF-EBS after each shutdown of the accelerators²¹. The provisional plan of that MDT is available in Appendix.

Lifetime optimizations using Badger

Contrary to the initial attempt using ES, the software Badger²² developed at SLAC has demonstrated to be extremely easy to set up, flexible to use and user friendly. It provides access to the Xopt algorithm library²³. We present below the user experience and the experimental results achieved thanks to the use of Badger and Xopt at the ESRF-EBS and DESY PETRA III storage rings. More details about the studies may be found in a recent publication in the ICALEPCS 2023 conference in Cape Town²⁴.

Xopt

Xopt is a high-level python package developed at SLAC National Accelerator Laboratory that provides a simple to use framework for connecting black box optimization algorithms with arbitrary optimization problems. Xopt decomposes optimization problems into three key components: defining

²⁰ Zhe Zhang, <https://github.com/slaclab/Badger>

²¹ N. Carmignani, et al., Online Optimization of the ESRF-EBS Storage Ring Lifetime, Proceedings of IPAC22, Bangkok, Thailand, 2022, doi = 10.18429/JACoW-IPAC2022-THPOPT001

²² Z. Zhang et al., “Badger: The Missing Optimizer in ACR”, Bangkok, Thailand, 13, 2022, paper TUPOST058, pp. 999–1002. doi:10.18429/JACoW-IPAC2022-TUPOST058

²³ R. R. et al., “Xopt: A simplified framework for optimization of accelerator problems using advanced algorithms”, in Proc. IPAC’23, Venezia, 2023, pp. 4796–4799. doi:doi:10.18429/jacow-ipac2023-thpl164

²⁴ S.Liuzzo et al., “Optimisation of the Touschek Lifetime in Synchrotron Light Sources Using Badger”, Cape Town, South Africa, 2023, paper MO3AO01, being published



parameter spaces and objectives, specifying how to evaluate these objectives, and implementing optimization algorithms.

The VOCS class defines the optimization space, including the variables, objectives, constraints and constants (statics). The Evaluator class defines how to evaluate objectives and constraints given points passed to it using serial or parallel (multithreading, MPI etc.) processes.

Finally, the Generator class implements the optimization algorithm, and is used to generate points in variable space to be evaluated. The main Xopt object choreographs the execution and communication between these three modules in order to perform an optimization cycle with the `step()` command.

This modular, object-oriented approach enables easy modification and customization of optimization routines for specific use cases. For example, the same optimization algorithm can be applied to both simulation and experiment, or shared between different accelerator facilities by swapping out the Evaluator object. On the other hand, generators can also be swapped out to compare the performance of different algorithms on the same optimization problem.

These objects can also be subclassed to customize evaluation or generation of points to solve specific problems. Optimization algorithms are defined by Generator objects, which are used to generate future points to be evaluated by calling their `generate()` method.

While users are free to implement their own optimization algorithms, Xopt comes pre-packaged with a number of conventional and advanced optimization algorithms tuned by experts to be applicable to a wide variety of optimization problems "off-the-shelf". Currently these algorithms include:

- Autonomous Characterization
 - Bayesian Exploration²⁵
- Single Objective Optimization
 - Nelder-Mead Simplex²⁶
 - Robust Conjugate Direction Search²⁷
 - Extremum Seeking²⁸
 - Upper Confidence Bound BO²⁹

²⁵ R. Roussel et al., "Turn-key constrained parameter space exploration for particle accelerators using bayesian active learning", *Nature Communications*, vol. 12, no. 1, p. 5612, 2021. doi:10.1038/s41467-021-25757-3

²⁶ J. A. Nelder and R. Mead, "A Simplex Method for Function Minimization", *The Computer Journal*, vol. 7, no. 4, pp. 308–313, 1965, Publisher: Oxford Academic. doi:10.1093/comjnl/7.4.308

²⁷ X. Huang, J. Corbett, J. Safranek, and J. Wu, "An algorithm for online optimization of accelerators", *NIM-A*, vol. 726, 2013. doi:10.1016/j.nima.2013.05.046

²⁸ B. Veglia et al., "Extremum seeking for accelerator optimisation", presented at IPAC'23, Venice, Italy, May 2023, MOPA137

²⁹ N. Srinivas, A. Krause, S. M. Kakade, and M. Seeger, "Gaussian process optimization in the bandit setting: No regret and experimental design", *arXiv preprint arXiv:0912.3995*, 2009. doi:10.48550/arXiv.0912.3995



- Expected Improvement BO³⁰
- Trust Region BO (TuRBO)³¹
- Multi-fidelity BO ³²
- Multi-Objective Optimization
 - Continuous NSGA-II³³
 - Expected Hypervolume Improvement BO ³⁴
 - Multi-Generation Expected Hypervolume Improvement BO ³⁵
 - Multi-Fidelity Expected Hypervolume Improvement

These generators can be used or modified via Python code inside or outside of Xopt. The Xopt framework has already been used at a wide number of accelerator facilities and institutions including LCLS, LCLS-II, FACET-II, Cornell University, University of Chicago, LBNL, AWA and DESY.

Badger

The Badger package enables the utilization of Xopt for real-time accelerator tuning by offering both graphical user interface (GUI) and command-line interface (CLI) for experiment operators. A view of the Badger *run monitor* panel during a single objective optimization is presented in Fig. 16.

³⁰ D. Zhan and H. Xing, “Expected improvement for expensive optimization: A review”, *Journal of Global Optimization*, pp. 1–38, 2020. doi:10.1007/s10898-020-00923-x

³¹ D. Eriksson, M. Pearce, J. Gardner, R. D. Turner, and M. Poloczek, “Scalable global optimization via local bayesian optimization”, *Advances in neural information processing systems*, vol. 32, 2019. doi:10.48550/arXiv.1910.01739

³² F. Irshad, S. Karsch, and A. Döpp, “Expected hypervolume improvement for simultaneous multi-objective and multi-fidelity optimization”, *arXiv preprint arXiv:2112.13901*, 2021. doi:10.48550/arXiv.2112.13901

³³ K. Deb, A. Pratap, S. Agarwal, and T. Meyarivan, “A fast and elitist multiobjective genetic algorithm: NSGA-II”, *IEEE Trans. Evol. Comput.*, vol. 6, no. 2, pp. 182–197, 2002. doi:10.1109/4235.996017

³⁴ S. Daulton, M. Balandat, and E. Bakshy, “Differentiable Expected Hypervolume Improvement for Parallel Multi-Objective Bayesian Optimization”, *Advances in Neural Information Processing Systems*, vol. 33, 2020. doi:10.48550/arXiv.2006.05078

³⁵ M. Song, X. Huang, L. Spentzouris, and Z. Zhang, “Storage ring nonlinear dynamics optimization with multi-objective multi-generation Gaussian process optimizer”, *Nucl. Instrum. Methods Phys. Res., Sect. A*, vol. 976, p. 164 273, 2020. doi:10.1016/j.nima.2020.164273





Figure 16: Badger application run monitor panel. The objective of minimization is displayed in the top plot, while the relative change of the parameters used for tuning is presented in the bottom plot. Users can easily customize the plotting preferences at any time through the toolbar, including options like using time as the x-axis instead of the iteration index or displaying normalized values of the variables.

Badger establishes connections between the generators (optimization algorithms) in Xopt and the underlying machine through its custom *interface* (which handles low-level and fundamental communication with the control system) and *environment* (containing optimization-related information about the machine, such as variables, tuning ranges, and observables). It provides a user-friendly GUI that allows users to easily fine-tune optimization properties, including selecting tuning knobs, configuring tuning ranges, and defining objectives and constraints.

Users can monitor the optimization progress through Badger's *run monitor*, available in both GUI and CLI modes. Furthermore, run data is automatically archived in databases after each iteration of the optimization to ensure no data loss.

Work done to prepare the optimization MDT with Badger

Dedicated Badger interfaces were prepared for EBS (TANGO control system) and PETRA III (TINE control system).

Several dedicated environments were created to reproduce the existing tuning techniques for EBS and PETRA III:

- (EBS) skew quadrupoles for vertical emittance tuning (used only for first test and to debug the code in the EBS-simulator)
- (EBS) sextupole knobs for lifetime or losses optimization
- (EBS) octupole knobs for lifetime or losses optimization



- (EBS) sextupole and octupole knobs for lifetime or losses optimization ³⁶
- (PETRA III) four skew quadrupoles QS1, QS2, QS3, QS4 for coupling plus the main quadrupoles in the FODO arc QF and QD (lifetime as observable)
- (PETRA III) 8 skew quadrupoles in wiggler sections to affect vertical dispersion (lifetime as observable)
- (PETRA III and EBS) transfer line booster to storage ring elements for injection efficiency (optimal injection conditions)
- (EBS) storage ring sextupoles and octupoles for injection efficiency (Dynamic aperture)

For both storage rings (EBS and Petra III) the observable is lifetime. However, at ESRF the target is to increase lifetime with sextupoles, while at PETRA III the objective is to reduce lifetime to obtain a smaller vertical beam size. In both cases the current decay during measurement must be taken into account. Following the Touschek Lifetime dependency with current the lifetime is normalized as follows:

$$\tau^{norm} = \tau(t) \frac{I(t)}{I_0}$$

The lifetime is estimated in PETRA III from a fit of the current decay or from the BPM sum signal with appropriate normalizations. At EBS, beam loss detectors are available and give much faster and reproducible data. A similar normalization is applied.

Concerning injection efficiency optimization, adequate functions were set up both at PETRA III and EBS to trigger injection and acquire injection efficiency data. Those were then included in a Badger environment and used for optimizations.

Lifetime optimizations for EBS

Lifetime optimization is performed routinely for EBS, to recover the best possible lattice performances before User Service Mode (USM).

The procedure for lifetime maximization is the following:

1. set all sextupole and octupole correctors to zero (periodic lattice)
2. kill any beam
3. cycle all magnets
4. refill uniform, 200 mA
5. open all insertion devices and collimators
6. set vertical scrapers to ± 4 mm
7. correct tunes and start fast and slow orbit correction feedbacks
8. start 10pm vertical emittance feedback
9. **optimize**: run sextupole and octupole knobs optimization
10. save settings, kill beam, cycle

³⁶ N. Carmignani et al., "Online Optimization of the ESRF-EBS Storage Ring Lifetime", Bangkok, Thailand, 13, 2022, pp. 2552–2555. doi:10.18429/JACoW-IPAC2022-THPOPT001



11. refill uniform, 200mA
12. measure Touschek and Vacuum Lifetime

At ESRF step **optimize** is usually done with the *run-by-hand* script mentioned above. This script scans the amplitude of each knob in a sequence, fits a parabola to the acquired data and keeps the amplitude producing the least total losses as measured by the 128 beam loss monitors around the SR.

With Badger/Xopt it was possible to easily replace this empiric sequential scan with more sophisticated algorithms.

The algorithms that were tested are:

- Nelder-Mead Simplex (on 26th March 2023)
- Upper Confidence Bound Bayesian Optimization (on 26th March 2023)
- Trust Region Bayesian Optimization (TuRBO) (on 27th August 2023 and all following measurements)

Other algorithms such as RCDS are available within Badger but there was no time to test them in the control room.

The whole procedure described above is repeated identically for each algorithm. Figure 17 summarizes the results of the optimizations in terms of lifetime and time to converge.

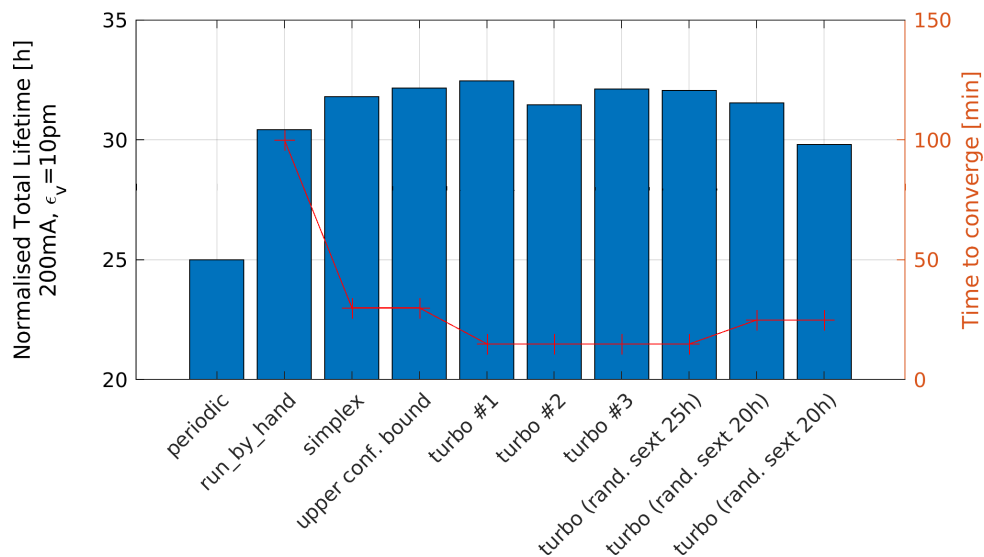


Figure 17: Total beam lifetime (Vacuum and Touschek lifetime contributions) and time to converge for different sextupoles and octupole settings. The label (periodic) corresponds to the absence of corrections on sextupoles and octupoles. All other bars represent different optimizations performed. All values are normalized for total current and vertical emittance.



All optimizers tested improved the maximum lifetime, compared to the periodic settings and to the results of the standard optimization procedure.

The empiric run-by-hand tuning takes about 100 minutes yielding about 30 hours lifetime.

The simplex and upper confidence bound algorithms take about 30 minutes before convergence and yield a lifetime of about 32 hours.

The TuRBO algorithm outperforms all other algorithms tested, by converging in only 15 minutes to total lifetime values above 32 hours.

Setting the sextupole and octupole strengths values found by the best run of optimizations in the storage ring led to the record Touschek lifetime values of 41 hours, achieved only once before for EBS in May 2021.

Lifetime optimizations for PETRA III

Two PETRA III environments were written specifically for the lifetime optimization experiment. The first one allows to act on the four skew quadrupoles QS1, QS2, QS3, QS4 which affect the machine global coupling (QS1 and QS4 for the difference resonance, QS2 and QS3 for the sum resonance). Also influencing the lifetime are the horizontal and vertical tunes. They are set by acting on the main quadrupoles in the FODO arc: QF and QD. For a more extended optimization the vertical dispersion in the damping wigglers is adjusted. This can be set through the second environment, where the vertical dispersion is corrected in the wiggler sections by varying the current in 8 skew quadrupoles located in the North and West ring sections. Similarly, as in the EBS case, the environments also set the boundaries within the optimization algorithms

can vary the magnet values, in order to avoid damages to the machine. The observable to be optimized also needs to be defined in the environment. The objective function used for the optimization was the normalized lifetime as previously mentioned.

The current optimization routine in PETRA III evaluates the operational values of QS1-4 by moving the tunes to the $Q_x - Q_y$ difference resonance and trying to achieve the smallest tune difference as possible and is typically done a few times per year, mostly during startup after a shutdown. The set-points of the main quadrupoles QF and QD are manually tuned to achieve at the same time a good injection efficiency and a small horizontal emittance (near the design value of the natural emittance). The optimal currents for the skew quadrupoles in the North and West sections are computed from the inverse dispersion response matrix obtained by measurements. This process is usually performed every week.

The Badger optimization test was performed in a dedicated machine development shift in March 2022 using a filling pattern of 10 bunches with a total current of 25 mA. Four different tests were performed acting on different sets of magnets.

- In the first case the lifetime was perturbed by setting the current in QS1, QS4 to 10 A and QS2, QS3 to 0 A. The currents in the same magnets were the optimization parameters.
- After observing that QS2 and QS3 had minimal impact on the lifetime a second test used QS1, QS4 together with the main quadrupoles QF and QD.



- For the third test the currents of the skew quadrupoles in the damping wigglers section was set to 0 to increase the lifetime and the optimization was performed initially using subsets of those quadrupoles (first the 4 in the West sector and then the 4 in the North sector).
- Lastly the optimization was performed tuning the 8 skew quadrupoles at the same time.

For all of the tests above the optimization used the BOtorch algorithm and the procedure followed was:

1. The current in the magnets was modified till a consistent increase in the lifetime was observed.
 2. The Badger optimization program was let to run till convergence.
 3. The obtained lifetime was compared with the one of the magnets configuration at step 1 and with the operational values, in each case correcting the electrons orbit with the customary routine before acquiring the measurement.
- The final test used the simplex algorithm to tune the eight skew quadrupoles starting the run from the operational values (instead of 0 as in the third test). No improvement was observed in the minimization, suggesting that the operational settings are optimal.

Figure 18 summarizes the results of the optimizations comparing the normalized lifetime with the one induced by the perturbed magnets settings and the operational one.

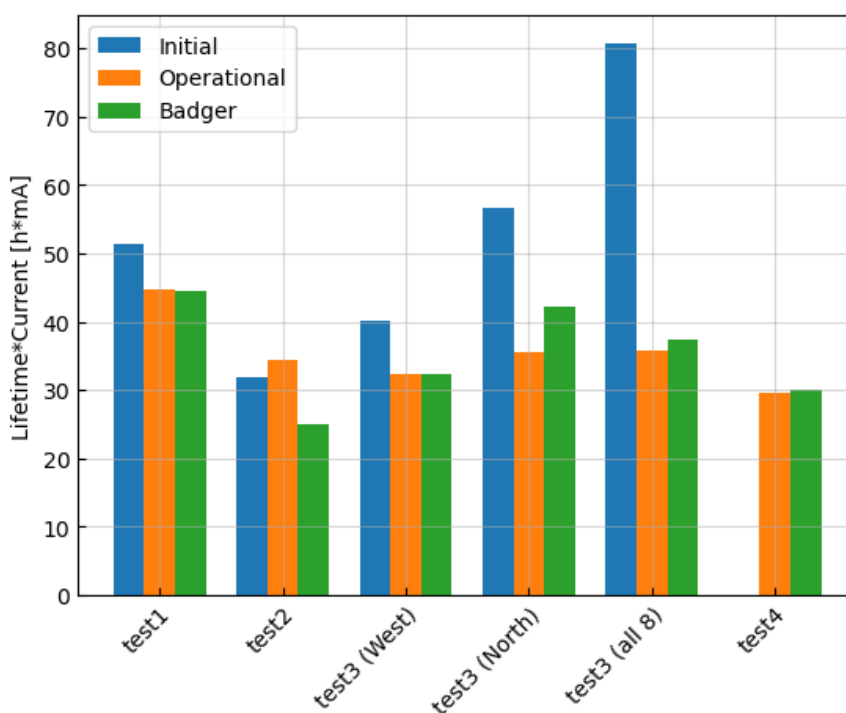


Figure 18: Comparison of the lifetime normalized with the current for the different tests performed in PETRA III. The blue bar represents the value obtained by detuning the relevant parameters from the operational value (in orange). The green bar is the value reached at the end of the Badger optimization. In the last test the optimization was performed from the operational values.

Injection efficiency optimizations for EBS

The use of badger for injection efficiency optimizations was twofold. On one side the magnets of the transfer lines allow to improve the injected beam position and optics. On the storage ring side, sextupoles and octupoles can be modified: in this case the injection efficiency increase is linked to increased dynamic aperture.

The results of such tuning for EBS are shown in Figure 19.

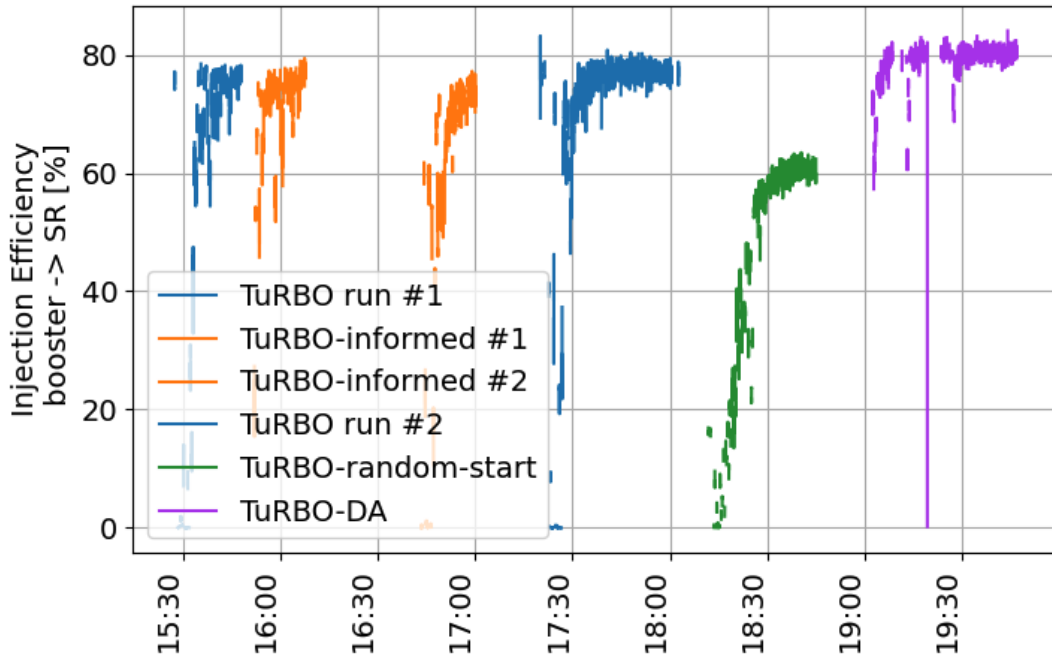


Figure 19: Injection efficiency during the optimizations performed with Badger and Xopt.

The first 3 series of points are simply tests. The last 3 are instead the interesting cases:

- 1) starting at ~17.30 optimization of transfer line elements reaching +2% injection efficiency compared to previous optimum;
- 2) starting at ~18.15 optimization of transfer line elements starting from random magnets set points. In this case a local minimum is found by TuRBO. An upper confidence bound algorithm will be tested in the future.
- 3) starting at ~19.00 optimization of SR sextupoles and octupoles. Dynamic aperture was increased leading to +2% injection efficiency. The lifetime of this setting was checked and did not appear reduced, as the sextupole and octupole combinations used for optimization were selected to affect only DA and not Lifetime.

A net gain of about 4-5% was obtained thanks to the use of Badger and Xopt.

Injection efficiency optimizations for PETRA III

The transport line E-Weg extends from the extraction septum in DESY II to the injection septum in PETRA III, and transports electrons at a beam energy of 6.0 GeV. Badger was used for adjusting the



current of a corrector in the horizontal (called IME186) and one in the vertical plane (SVE178) of the E-Weg maximizing the injection efficiency. The optimization algorithm used was simplex, allowing the parameters to be varied within ± 1 A relative to nominal values.

After 20 steps, which took about 10 minutes, the injection efficiency was increased by 13% as shown in Figure 20 below.

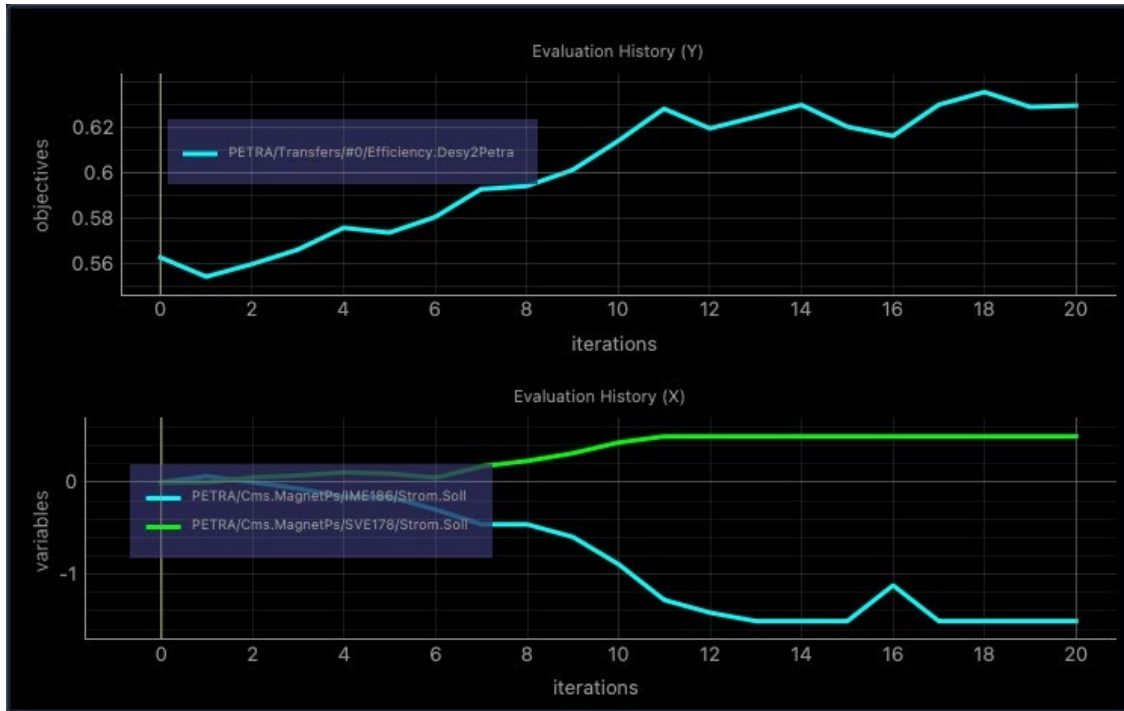


Figure 20: Injection efficiency optimization performed with Badger in PETRA III.

Conclusions about the MDT activities at EBS and PETRA III

Badger has been successfully used at EBS also for local optimization of sextupoles about a newly installed undulator and to optimize the lifetime after the installation of new magnets.

The Xopt TuRBO algorithm reached an optimal tuning configuration seven times faster than conventional scanning algorithms and more than fifty times faster than a human operator (assuming 2x8h shifts of manual tuning).

Badger has been set up at EBS with the Xopt TuRBO algorithm and is now available for operators to be used during user service mode for lifetime optimizations. In fact, the optimization process is sufficiently fast and sensible (requires very small magnet setting variations), to be completely transparent for user operations (except the improved lifetime performances).



For PETRA III the use of Badger did not exceed the classic operation tuning and it is thus kept for machine studies only and as a valuable tool for the PETRA IV upgrade project³⁷.

Future use of Badger and Xopt will continue the studies started on injection efficiency optimization including additional parameters (such as the booster sextupoles at extraction) and testing different algorithms available in Xopt. Also, multi-objective optimizations will be soon possible with Badger, allowing simultaneous lifetime and injection efficiency optimisation for instance.

Measurement and analysis of TbT data analysis to determine Storage ring optics

The correction of the linear optics is very important to operate the synchrotron light sources reliably, with good lifetime and good injection efficiency. Most of the light sources measure the linear optics and compute the corrections by fitting the orbit response matrix (ORM). This is a standard technique and it is used both at the ESRF and at DESY.

Alternatively, to the orbit response matrix measurement, the linear optics can be obtained from the analysis of the turn-by-turn (TbT) signals from the beam position monitors (BPMs) when the beam is excited with an oscillating dipole magnet (AC-dipole). This technique is used in colliders as LHC³⁸ but also in some light sources, as PETRA III in DESY³⁹.

Turn by turn data with betatron oscillations can be obtained with a single turn kicker. In that case, the oscillations become quickly decoherent because of non-zero chromaticity and non-zero detuning with amplitude. If the decoherence is small, because the chromaticity and the detuning with amplitude are small, the oscillations are damped by the synchrotron radiation in a few tens of ms. The TbT and ORM methods were compared in ESRF's predecessor of EBS⁴⁰.

An AC-dipole can create a stable oscillation at large amplitude without decoherence. Optics measurements with TbT analysis of the oscillations driven by an AC-dipole have the advantage of being much faster than the orbit response matrix measurement. The precisions obtained with the two techniques are comparable.

Sample TbT-based optics measurement in PETRA III

In Petra III, the beam may be excited in all three directions using Multi-bunch feedback stripline kickers and cavities. Figure 21 shows a typical frequency spectra of such an excitation.

³⁷ I. V. Agapov et al., "PETRA IV Storage Ring Design", Bangkok, Thailand, 13, 2022, pp. 1431–1434.
doi:10.18429/JACoW-IPAC2022-TUPOMS014

³⁸ R.Tomas et al., LHC optics measurement and correction software progress and plans,
<https://doi.org/10.18429/JACoW-IPAC2019-WEPGW116>

³⁹ A.Kling, Turn-by-turn data analysis for PETRA III, IPAC 2010, WEPEA017

⁴⁰ L.Malina et al. , Improving the precision of linear optics measurements based on turn-by-turn beam position monitor data after a pulsed excitation in lepton storage rings,
<https://journals.aps.org/prab/abstract/10.1103/PhysRevAccelBeams.20.082802>



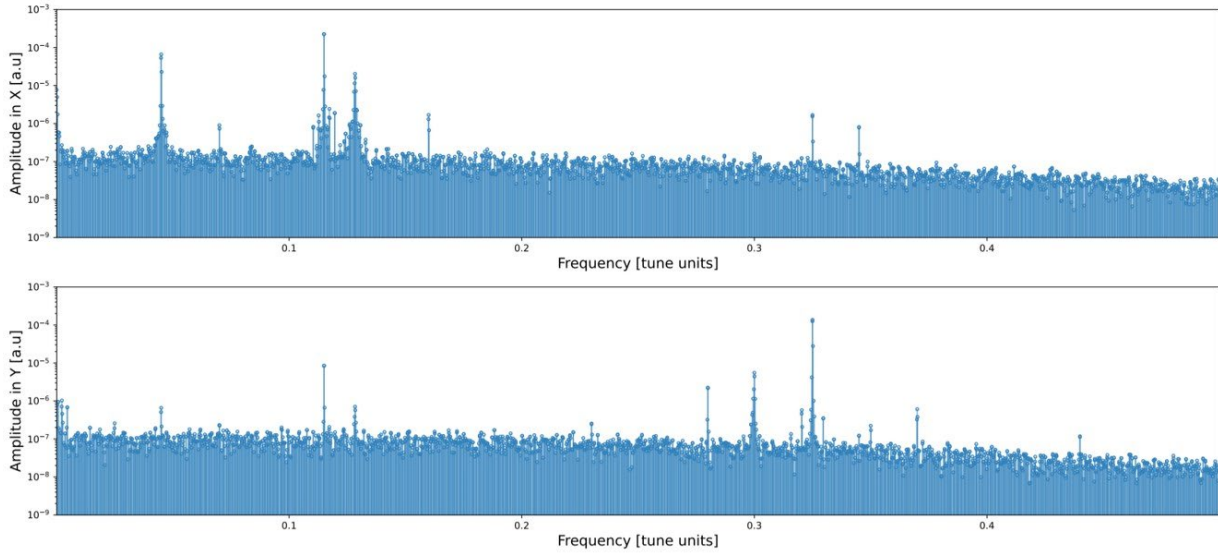


Figure 21: Frequency spectra of BPM TbT data in horizontal plane (top plot) and vertical plane (bottom plot). Note the “driven” spectral as well as beams “natural” lines.

The typical measurement based on a single excitation lasting for 25000 turns measures total phase advance beating shown in Figure 22, dispersion beating shown in Figure 23, and Coupling Resonance Driving Terms (RDT) shown in Figure 24 (only difference resonance).

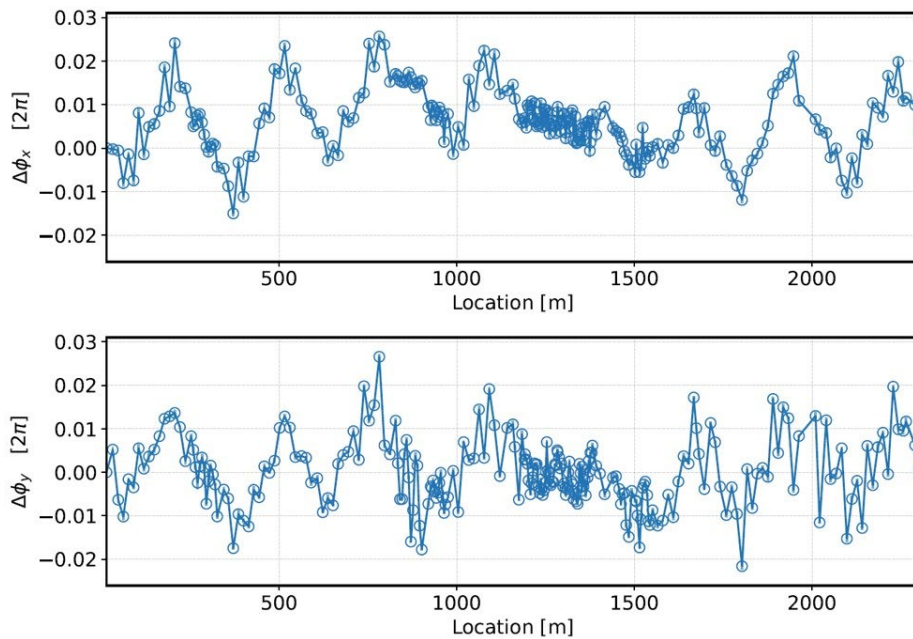


Figure 22: Typical total phase advance beating with respect to model values measured in PETRA III

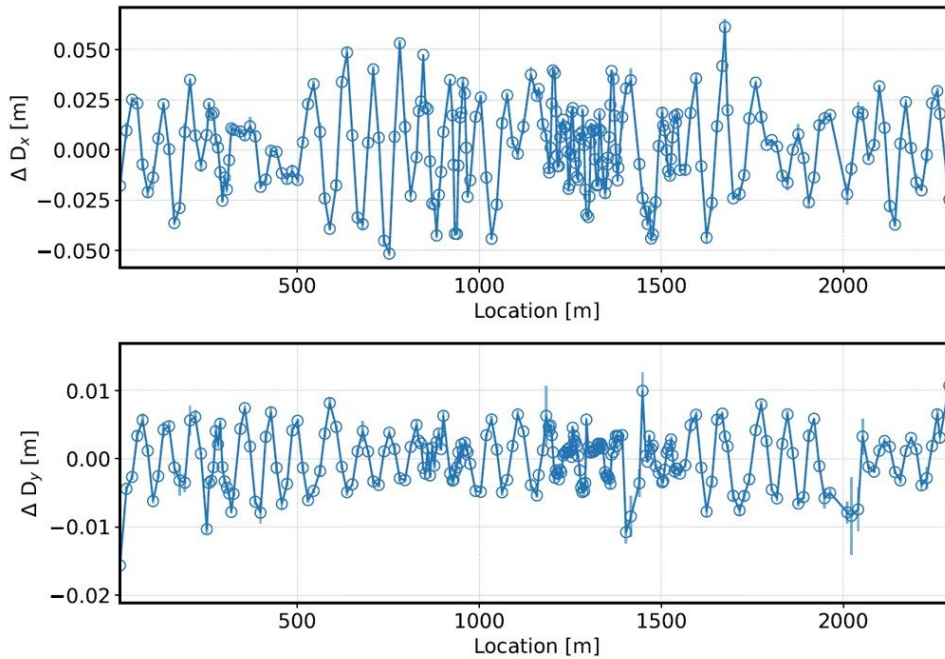


Figure 23: Typical dispersion beating with respect to model values measured in PETRA III

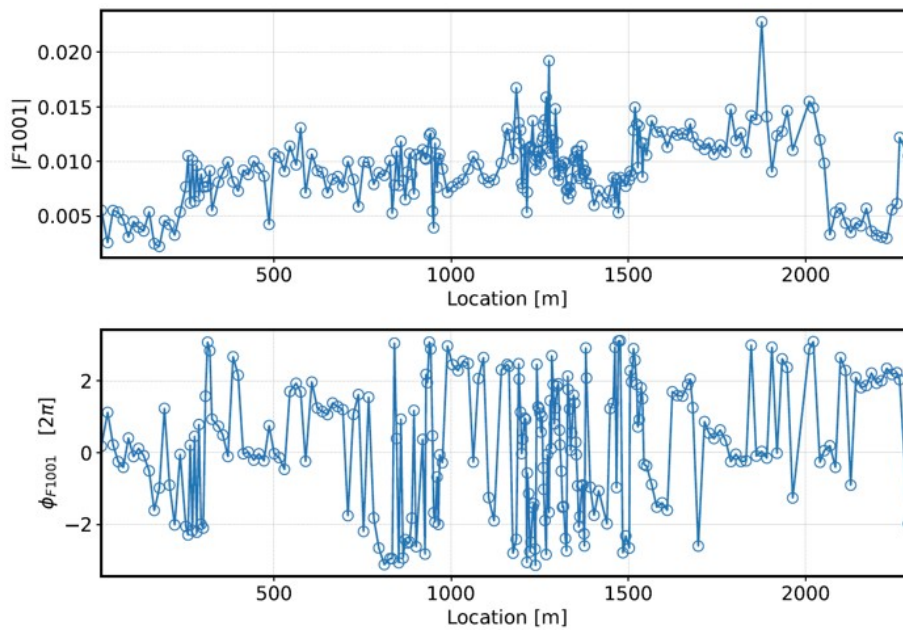


Figure 24: Typical difference resonance driving term measured in PETRA III

Work done to prepare the MDT

A magnetic shaker is installed in the ESRF storage ring and it is used to blow-up the emittance of the beam using a white noise. The AC-dipole excitation is obtained by sending a sinusoidal signal at a specific frequency, close to the betatron tune, to the magnetic shaker. The magnetic shaker used as an AC-dipole has been tested before the MDT.

A procedure to switch the BPM to TBT acquisition mode has been prepared by the diagnostics group and has been tested before the MDT. The aim of this procedure is that the BPMs are all synchronized and don't mix the signal from two consequent turns.



The Optics Measurements and Corrections (omc3⁴¹) python code to do the analysis has been developed at CERN and is used in several machines, for example, at PETRA III. Before the MDT, the code has been installed at ESRF and it has been tested in simulations. The ESRF lattice has been converted in MAD-X format to be compatible with the omc3 code. The analysis parameters of the ESRF lattice have been defined within omc3 and are subject to further tuning.

Description of the MDT activity

An MDT shift on November 7th 2022 was booked to try the analysis of the TBT signal with the AC-dipole at the ESRF.

The amplitudes and frequencies of the AC-dipole were tuned to have a good TBT signal, similar to the ones tested in simulations.

The filling pattern of the machine had to be short enough in order to avoid issues with BPM synchronization and to limit the excitation phase difference for the different bunches (see fig. 25). With 100 bunches, the phase difference inside the train was considered negligible.

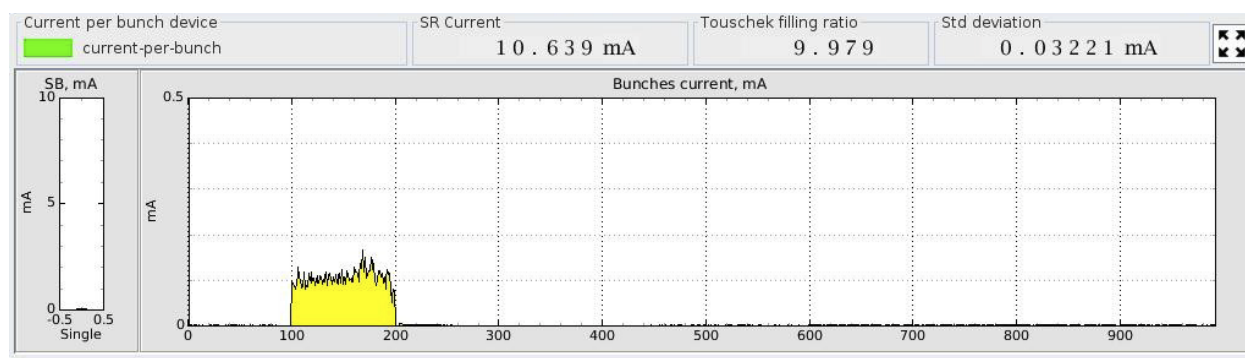


Figure 25: Filling pattern used in the ESRF storage ring for the AC-dipole MDT.

The TBT data were acquired for about 50000 turns and many different acquisitions were performed, varying the total current, the filling pattern, the amplitude and the frequencies of the excitation. In the currently best conditions, the beta functions could be measured from the frequency analysis of the TBT data with about 5 to 10% error rms (Fig. 26). This is still not at the acceptable level, so more studies have to be performed to better understand the reasons for the low accuracy. Certainly, the analysis parameters have to be optimized for the ESRF lattice.

⁴¹ <https://github.com/lmalina/omc3>

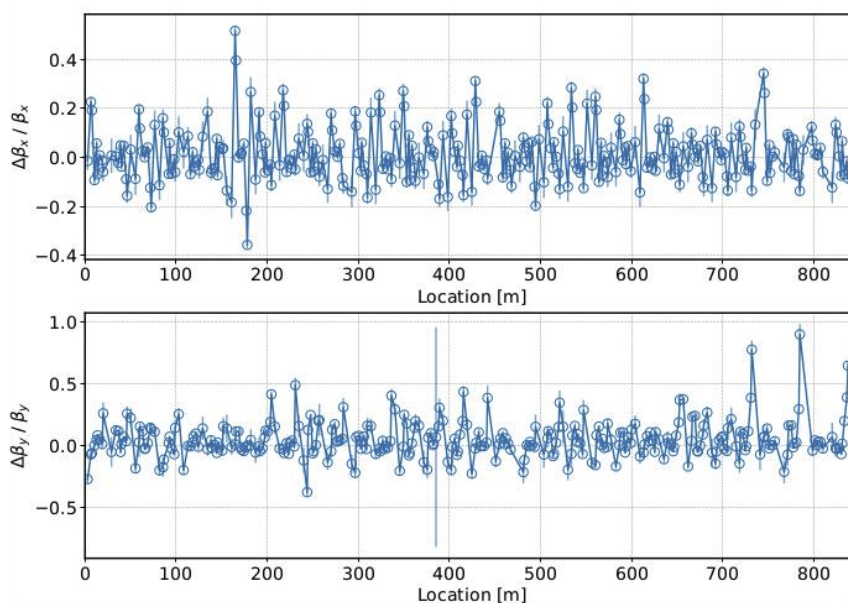


Figure 26: Beta beating measurement with TBT analysis.

Results and outlook

The accuracy of the measurement of the beta function at the ESRF with the analysis of the BPM TBT signal with AC-dipole excitation is currently not at the level of the orbit response matrix, so further studies (both in simulation and experimental) are planned to better understand the problem.

Definition of a new functions for errors and correction based on pyAT

Commissioning simulations are mandatory for any new storage ring (SR) design. Running such simulations allows defining the procedures to achieve first turns, accumulation and finally low emittance tuning and optics corrections. Once all the correction steps are tuned and optimized these commissioning simulations show if the SR under study will be able to reach its design performance in terms of injection efficiency (IE) and Touschek lifetime (TL). Commissioning simulations are thus mandatory for any SR not only to define the final performances in presence of realistic errors but also to evaluate maximum tolerated errors, to choose the optimal commissioning correction sequences and to assess the loss/gain in DA, IE, TL of optics adaptations performed while operating the SR.



Tools for commissioning simulations are available based on several codes (among others see ⁴² and ⁴³), but it is often difficult to adapt to other SRs. Recently Simulated Commissioning (SC)⁴⁴ has been introduced to the community based on matlab accelerator toolbox (AT)⁴⁵.

Work has been carried out in the framework of the present project to provide a set of tools for commissioning simulations also for the python version of AT.

Implementation of a pyAT based commissioning simulation toolkit

The actions expected from a commissioning simulation toolkit are rather basic:

- 1) set errors based on a given error table to generate N possible realistic SR scenarios
- 2) correct lattice
- 3) compute relevant quantities (DA, IE, MA, etc...)
- 4) visualize a summary of the results

The software tools developed (available for download here:

<https://gitlab.esrf.fr/BeamDynamics/commissioningsimulations>) are designed considering also the following specifications:

- simple definition of errors and corrections to apply: python dictionaries.
- Modular structure (each component of the code is stand-alone. Other parts of the code may be added easily, as plugins)
- Tests / example / demos available for each submodule and for the overall usage
- Parallel computation (multiprocessing)
- SLURM cluster submission (parallel / distributed computations)
- Organized folders, easy to add seeds, easy to retrieve data
- Possible to skip/postpone DA/MA for correction loop optimization
- 6D tracking, with radiation and RF cavity managed by pyAT

⁴² S. Liuzzo, N. Carmignani, J. Chavanne, L. Farvacque, G. Le Bec, B. Nash, P. Raimondi, R. Versteegen, S. White, "Updates on Lattice Modeling and Tuning for the ESRF-EBS Lattice.", 7th International Particle Accelerator Conference, 10.18429/JACoW-IPAC2016-WEPOW005, WEPOW005, 2016

⁴³ Sajaev, V., "Commissioning simulations for the Argonne Advanced Photon Source upgrade lattice", PhysRevAccelBeams.22.040102, 10.1103/PhysRevAccelBeams.22.040102

⁴⁴ T. Hellert, C. Steier, M. Venturini "Lattice correction and commissioning simulation of the Advanced Light Source upgrade storage ring" PhysRevAccelBeams.25.110701, 10.1103/PhysRevAccelBeams.25.110701

⁴⁵ B.Nash, N. Carmignani, Farvacque, S. Liuzzo, T. Perron, P.Raimondi, R. Versteegen, S. White, (2015). NEW FUNCTIONALITY FOR BEAM DYNAMICS IN ACCELERATOR TOOLBOX (AT)



- use of analytic / semi-analytic / numeric computations
- flexible to changes of SR (centralized input of all machine dependent parameters)
- flexibility in the definition of the corrections to be applied
- speed of computations, making use of analytic formulas where possible
- easy python installation “pip install .”

A single configuration file holds all the lattice dependent information. This includes for example the location of correctors required for each step of the correction.

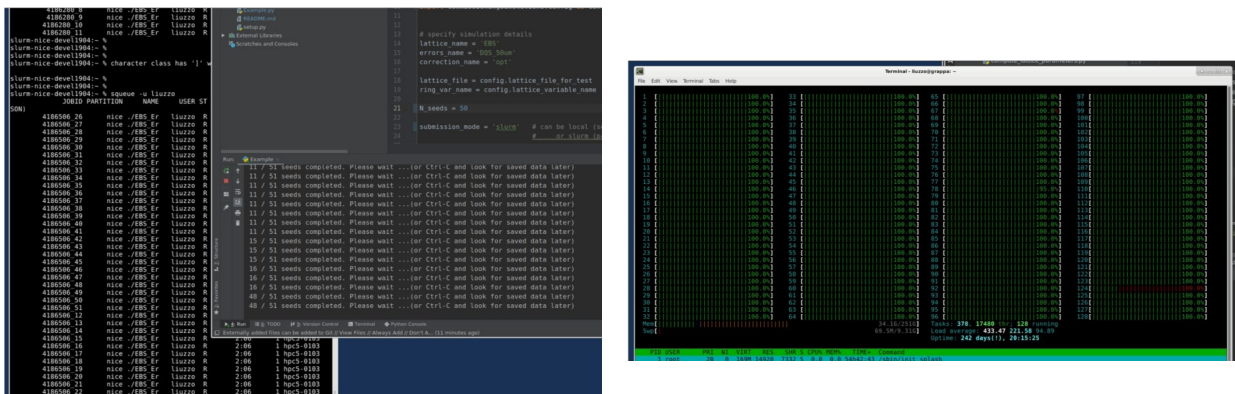


Figure 27: pyAT based software running (right) in a local 128 cores machine or (left) using a remote computing cluster.

A flag is used to switch between local and cluster computing. In the first case lattices are analyzed in series, and computations are done exploiting all available local computing resources. In the second case, a given number of processors is charged to analyze the N lattice seed. In this case also the lattice seeds are analyzed in parallel. The two options are kept in order to make the code usable also by laboratories where large computing clusters are not available. Figure 27 shows the code running in local mode or in cluster mode. The data produced by the code is organized in subfolders as depicted in Fig 28.

In order to speed up the tests, and in particular to choose and fine tune the correction scheme it is not necessary to compute DA, IE and MA. It is sufficient to look at basic lattice optics parameters such as orbit, tunes and optics. For this reason, the computation of DA, IE and MA may be excluded, with a significant gain in time (up to more than 90%).

All features of the pyAT tracking engine are inherited by the software. Full 6D tracking of electrons in presence of radiation, quantum diffusion and RF cavities may be performed by simply setting appropriately the input lattice.



Error setting is also based on the core pyAT. For the moment only the basic errors (alignment, gradient, rotation and BPM errors) are available, but work is ongoing on this topic and will be part of the next report.

```

├── Design                                # FOLDER of data for reference Lattice
│   ├── DATLTDesign.pkl                  # data of DA and LT
│   ├── DADesign.png                    # DA image
│   ├── LatticeDesign.pkl               # pyAT lattice file
│   ├── TLTDesign.png                   # MA image
│   └── LatticeDesignData.pkl           # optics parameters file
├── Matrices                              # FOLDER of data for response matrices
│   ├── TRM.mat                         # trajectory response
│   ├── ORM.mat                         # orbit response
│   ├── Jnumeric.mat                   # derivative of ORM for optics correction
│   └── ...
├── Seed000                              # FOLDER of data for Seed000
│   ├── Errors.pkl                      # errors assigned to this Seed 0
│   ├── Errors.txt                      # printed version of errors assigned to seed 0
│   ├── LatticeErrors.pkl               # pyAT lattice with errors in key rerr
│   ├── LatticeErrorData.pkl            # optics parameters file for lattice with errors
│   ├── LatticeCorrected.pkl            # pyAT lattice with errors and correction in key rcor
│   ├── LatticeCorrectedData.pkl        # optics parameters file for lattice with errors and correction
│   ├── DAErrors.png                   # DA image
│   ├── DATLTErrors.pkl                 # data of DA and LT with errors
│   ├── TLErrors.png                   # MA image with errors
│   ├── DACorrected.png                 # data of DA and LT with errors and corrections
│   ├── DATLTCorrected.pkl              # data of DA and LT with errors and correction
│   ├── DA_compare.png                 # DA image comparing design, errors and errors+correction
│   ├── TLTCorrected.png                # MA image with errors and correction
│   ├── ComparativeData.pkl              # data compared to Design
│   ├── ComparativeData.txt             # printed version of data compared to Design
│   └── MA_compare.png                  # MA image comparing design, errors and errors+correction
├── Seed002
├── Seed003                              # same structure as Seed000 folder
├── ...
├── Seed##
├── CorrectionParameters.pkl             # global correction parameters
├── params.txt                           # slurm submission file of parameters
├── sbatch.sh                             # slurm submission file
└── SummaryFigures                       # FOLDER of figures summarizing the above data
    ├── DA.png
    ├── LT.png
    ├── MA.png
    ├── Beta.png
    ├── COD.png
    ├── DISP.png
    ├── EMIT.png
    └── TUNE.png

```

Figure 28: pyAT commissioning simulations output folders structure. One folder per seed is present and one folder with the reference design values.

Correction using pyAT based commissioning simulation toolkit

The corrections available and tested are presently:

- First turns beam threading⁴⁶ (see Figure 29)
- closed orbit correction
- tune correction
- chromaticity correction
- error model fit based on closed orbit response matrix (LOCO like optics correction)
- optics correction⁴⁷ (see Figure 30)

⁴⁶ S M Liuzzo and N Carmignani and A Franchi and T Perron and K B Scheidt and E Taurel and L Torino and S M White, "Preparation of the EBS beam commissioning", Journal of Physics: Conference Series, IOP Publishing, 10.1088/1742-6596/1350/1/012022, 2019

⁴⁷ Simone Liuzzo, Nicola Carmignani, Lee Carver, Laurent Farvacque, Thomas Perron, et al.. HMBA Optics Correction Experience at ESRF. *12th International Particle Accelerator Conference*, May 2021, Online, Brazil. pp.TUPAB048, [10.18429/JACoW-IPAC2021-TUPAB048](https://doi.org/10.18429/JACoW-IPAC2021-TUPAB048)



- coupling correction
- normal and skew quadrupoles RDTs correction

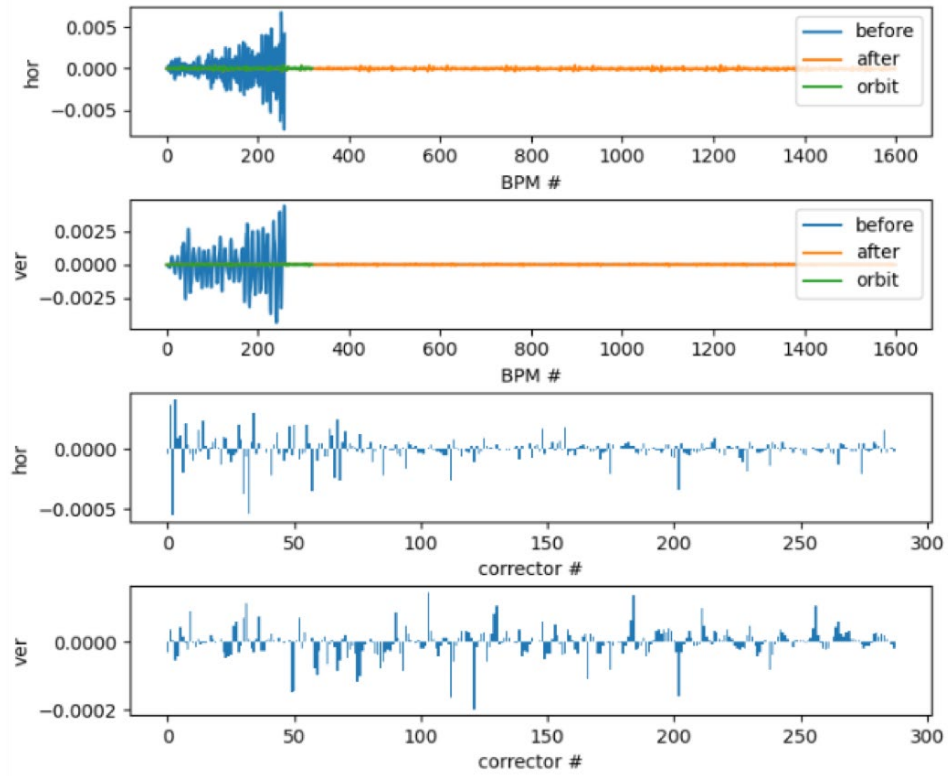


Figure 29: Trajectory correction to get first turns and beam accumulation

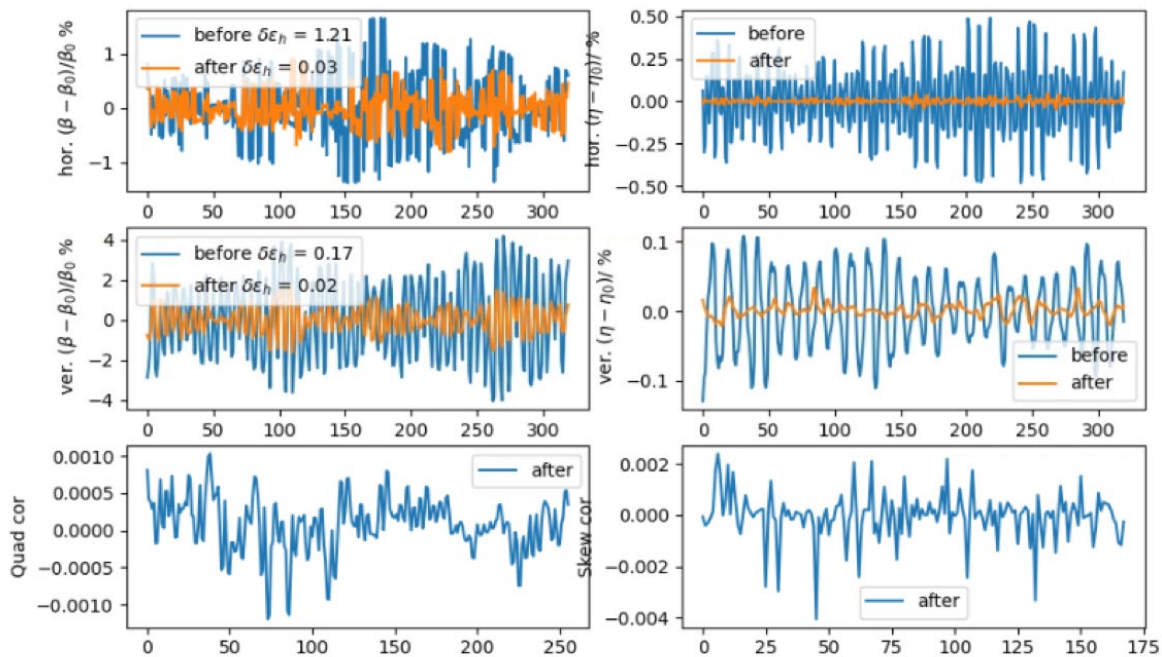


Figure 30: optics dispersion and coupling correction based on measured orbit response matrix fit.

In the near future also the following corrections will be added:

- BBA
- BBA from trajectory data
- NOECO⁴⁸
- tune from trajectory

These corrections may be done in any sequence and are fully tunable in all their parameters. A typical correction sequence executes the corrections in the order listed above and iterates a few times before considering the lattice converged.

Implementation and use of analytic formulas

Several steps of corrections require the computation of response matrices ahead (for example the response of orbit to a variation of each steerer magnet in the lattice). Those matrices are computed based on the design lattice and stored in files such to be available for individual parallel correction computations of each seed.

These computations, even if done only once, may be rather long, in particular those necessary for the optics correction that require to compute the response of orbit at every steerer in both planes and for

⁴⁸ D.K. Olsson, Å Andersson, M. Sjöström, "Nonlinear optics from off-energy closed orbits", Phys. Rev. Accel. Beams, 10.1103/PhysRevAccelBeams.23.102803



each normal and skew quadrupole in the lattice. Moreover, in some cases it is necessary to update these matrices during the correction, thus multiplying the number of long computations.

For this reason, the code took advantage of recent analytic results⁴⁹ to make such computations as fast as possible.

In particular, the equations presented in ⁵⁰ are implemented by making use of tick magnets corrections. This was never done before, and proved to be crucial to make the analytic formulas work correctly.

An example of the formulas introduced for Tune Response is given below (simplest case). The equation on the first row corresponds to the thin magnet approximation, the one on the second row to thick magnet corrections. K is the quadrupole gradient, L its length and α , β , γ are the Twiss optics parameters.

$$\frac{\Delta Q}{\Delta K_j} = \frac{\beta_j}{4\pi}$$

$$\frac{\Delta Q}{\Delta K_j} = \frac{\frac{1}{2} \left[\beta_j + \frac{\gamma_j}{K_j} \right] + \frac{\sin(2\sqrt{K_j}L_j)}{4\sqrt{K_j}L_j} \left[\beta_j - \frac{\gamma_j}{K_j} \right] + \frac{\alpha_j}{2K_jL_j} [\cos(2\sqrt{K_j}L_j) - 1]}{4\pi}$$

The formulas are tested against their numeric equivalent and show extremely good agreement when including thick magnet corrections for steerers and quadrupoles. In Figure 31 the numeric (reference) and analytic response matrices are compared.

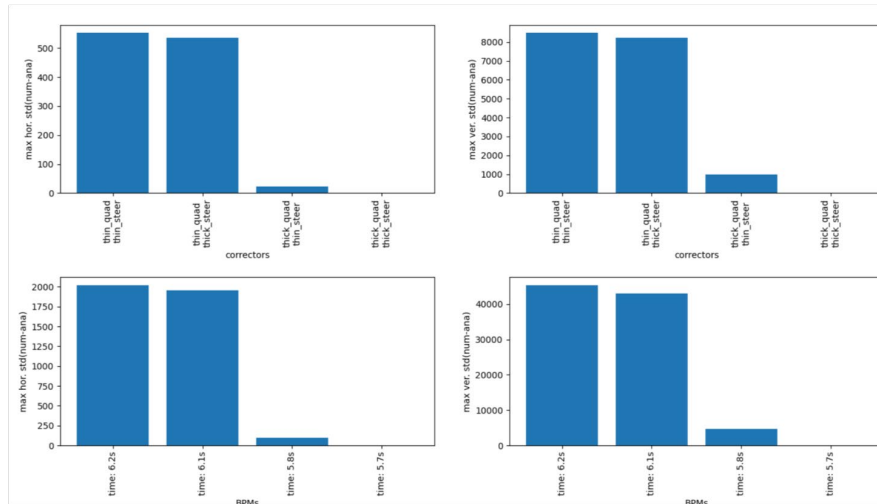


Figure 31: Comparison of the residual difference between analytic and numeric response matrices in several cases: without thick magnets corrections, with thick steerers corrections, with thick quadrupole corrections and with tick steerers and quadrupole corrections.

⁴⁹ <https://arxiv.org/abs/1711.06589v2>

⁵⁰ <https://arxiv.org/abs/1711.06589v2>



The use of these equations allows to significantly speed up the computations. Several tests were performed showing a gain of a factor ~ 8 in speed for equal computing power conditions (see Figure 32).

Publication of the above results is foreseen at the next IPAC 2023 conference in Venice.

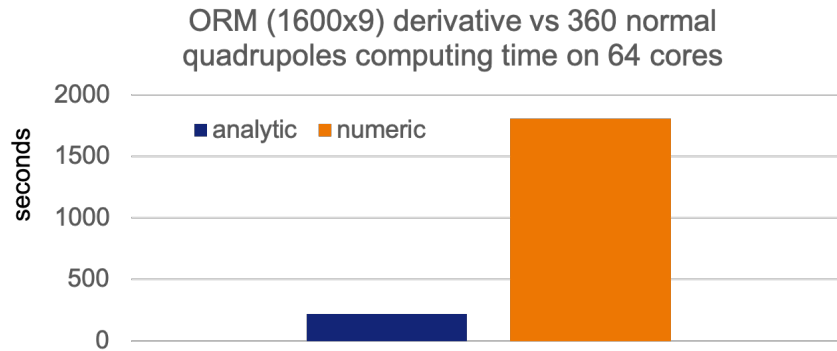


Figure 32: Numeric and analytic computation speed for a derivative of orbit response matrix (1600 Beam position monitors, 8 steerers, 360 quadrupoles) run in parallel on a 64CPUs AMD EPYC 7543 3.5 GHz processor.

Typical output of commissioning simulations in pyAT

The typical results of a full commissioning simulation in pyAT performed with the code developed in the framework of the EURIZON project are presented in Figures 33 and 34 for the EBS lattice.

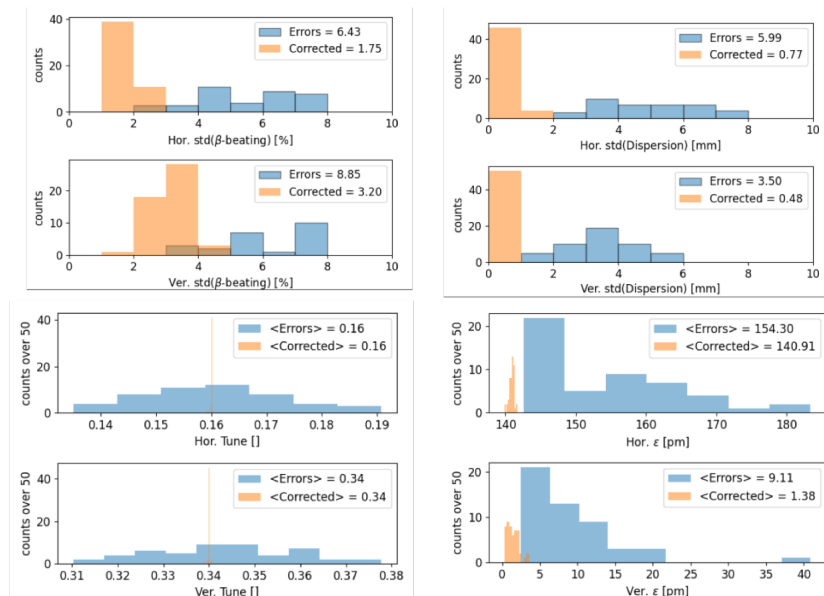


Figure 33: Optics parameters before and after correction for commissioning simulations of the EBS lattice



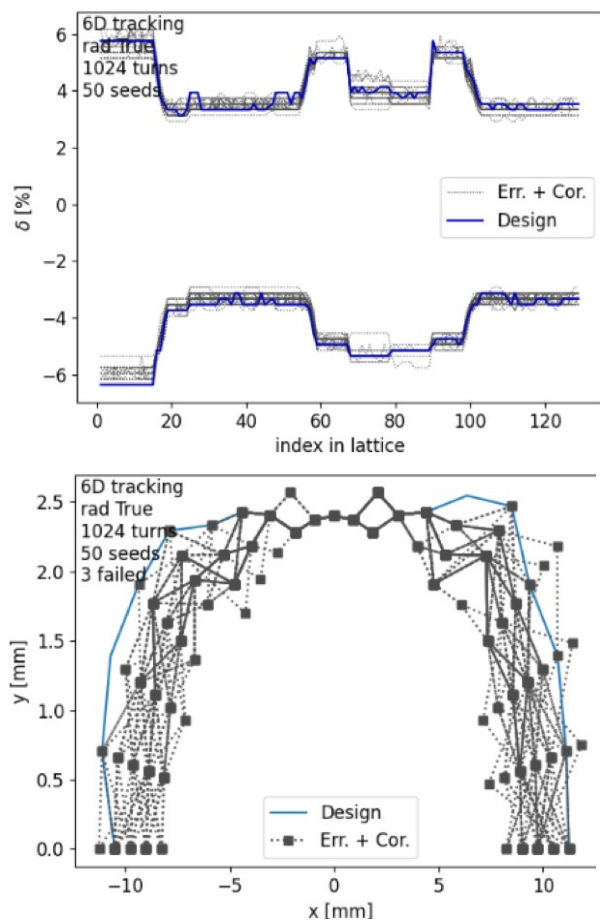


Figure 34: DA and MA after correction for commissioning simulations of the EBS lattice

The same software has presently been used for the EBS lattice⁵¹, ESRF-DBA lattice⁵², for the FCC-ee⁵³ collider lattice and for the PETRA IV lattice⁵⁴.

⁵¹ P. Raimondi, N. Carmignani, L.R. Carver, J. Chavanne, L. Farvacque, G. Le Bec, D. Martin, S.M. Liuzzo, T. Perron, S. White, “Commissioning of the hybrid multibend achromat lattice at the European Synchrotron Radiation Facility”, PhysRevAccelBeams.24.110701, 10.1103/PhysRevAccelBeams.24.110701

⁵² G. Chasman, K. Green and E.M. Rowe. “Preliminary design of a dedicated synchrotron radiation facility”, Technical report, United States, 1974

⁵³ K.Oide, S. Aumon, T. Charles, D. El Khechen, D. Shatilov, T. Tydecks “Several Topics on Beam Dynamics in FCC-ee”, 62nd ICFA Advanced Beam Dynamics Workshop on High Luminosity Circular e+ e- Colliders, 10.18429/JACoW-eeFACT2018-MOYAA01

⁵⁴ I. Agapov, R. Brinkmann, Y.-C. Chae, X. Gavalda, J. Keil, R. Wanzenberg, Rainer, “Lattice Design for PETRA IV: Towards a Diffraction-Limited Storage Ring”, 60th ICFA Advanced Beam Dynamics Workshop on Future Light Sources, 10.18429/JACoW-FLS2018-MOP1WB01, 2018



Several features are still under development and will be part of the next report:

- additional correction modules
- tests with other SR lattices
- extended errors, in particular large amplitude survey errors

Python simulated commissioning

After discussion with the concerned people the above code has been put in stale to focus on the development of a python version of Simulated Commissioning matlab software tools. The development began with translating the SC library into Python with the support of the Artificial Intelligence (AI) tool, ChatGPT.

Translation by ChatGPT

In the translation, ChatGPT's engine code-davinci-002 was used. Due to limitations on the length of prompts, the SC code was first stripped of all comments on separate lines. It was submitted to the engine along with a description of the input (Matlab code), the action (conversion) and the requested output (Python code) followed by the first lines of the assumed Python code, i.e. import numpy and matplotlib and define a function name. Figure 35 shows a code snippet applied to all files in the SC toolkit.

```
def remove_comments_in_file(ffile: str, source_dir: str = "") -> str:
    with open(f"{source_dir}{ffile}", "r") as mfile:
        lines = mfile.readlines()
        new_lines = [l.replace("\t", " ").strip("\n") for l in lines if not l.strip().strip("\t").startswith("%")]
        new_lines = [l for l in new_lines if l.strip("\t\n")]
        return "\n".join(new_lines)

def matlab_to_python(matlab_code: str, python_start: str = "") -> str:
    intro = "# Convert this from Matlab to Python:\n# Matlab version \n\n"
    ending = "\n# End\n# Python version\n\n"
    prompt = intro + matlab_code + ending + python_start
    response = openai.Completion.create(model="code-davinci-002", temperature=0, top_p=1, frequency_penalty=0,
                                       presence_penalty=0, max_tokens=len(prompt), stop=[intro[:20]], prompt=prompt)
    return python_start + response.choices[0].text
```

Figure 35: Code snippet to translate code using ChatGPT's Python API

Since the functions were translated one by one, and they contain calls to the other functions of SC toolkit, the signatures of translated methods needed to be adapted manually.

Library components

In this section, we discuss the data structures that store real and ideal lattices and the information on various sources of uncertainties. Later, the interfaces between real and ideal observation/settings are discussed and finally, available correction algorithms are listed.

Data Structures

In contrast to lattice design tools, software for error analysis and commissioning simulations must treat each lattice element as a unique entity.

Typical usage of the library proceeds through the following steps:



- Initialisation of the SimulatedCommissioning class,
- Definition and registrations of error sources,
- Generation of a machine realization including errors,
- Interaction with the machine.

After initializing the core structure, the user registers elements like magnets, Beam Position Monitors (BPMs) or cavities, including all the relevant error sources in the structure. It is important to note that the uncertainties are only stored in a dedicated structure at this step: the ideal and actual rings are still identical. When applying errors, the uncertainties are used to generate random error distributions, assigned as attributes of corresponding elements in the lattice.

The error sources currently available for inclusion in the commissioning simulation are the following:

- BPM Errors
 - Horizontal and vertical offsets,
 - Noise (closed orbit, turn-by-turn),
 - Roll around beam direction,
 - Calibration, i.e. scaling error (2D),
 - Sum error, i.e. error of the beam intensity measurement,
- Magnet Errors
 - Offsets in all three dimensions,
 - Rolls around all three axes,
 - Strength calibration,
 - Multipole errors (strength offsets and calibrations),
- Errors of three stackable types of support structures
 - Offsets in all three dimensions,
 - Rolls around all three axes,
- Errors of injected beam
 - Static errors (6D) present in every injection,
 - Injection jitter (6D), different shot to shot,
- RF phase, frequency and voltage errors
- Ring circumference errors

Real to ideal interface

The purpose of the software is to adjust lattice parameters, such as magnet strengths, to reach the operational state using mostly beam-based corrections. Once the real lattice was created, the errors were assigned. However, they also needed to be kept during the lattice correction. For example, a magnetic field does not lose a scaling error when the current is set to a different value. In this sense, errors are persistent differences (typically relative or absolute) between a set point value set by the user and the parameter used in the underlying beam dynamics simulations.

Such an interface is available to set normal and skew magnetic field components and RF-cavity properties.

The output from beam dynamics simulation, represented by tracking, features a similar interface for beam position monitor (BPM) reading. The interface covers several features:



- Averages trajectories/orbits of all tracked particles
- Offsets and rolls the orbit values
- Adds noise and sum signal errors. Note that in the trajectory case, the noise is inversely proportional to charge, i.e. if some of the particles are lost, the signals downstream will be noisier.

Only the interfaces mentioned earlier need to be modified to commission an already-built synchrotron, i.e. not in simulation. This is due to the design choice of strict separation of methods available to real machines and the analysis methods, which evaluate the performance of commissioning simulations.

Basic correction algorithms

Several important correction algorithms optimize the machine's performance and precisely control the beam's trajectory, orbit, RF settings and lattice optics, specifically, the following are presently available in pySC:

Trajectory correction The trajectory is iteratively acquired and corrected (via a response matrix approach) using the steerers upstream of the last BPM reached by the beam. After achieving first-turn transmission, an approximate one-turn closed orbit is searched by correcting the second-turn reading of the first several BPMs such that they are equal to their reading in the first turn.

RF setup The averaged trajectory at specified BPMs is logged turn-by-turn whilst the phase of RF is scanned (full 360\degree). The RF phase is set to a value for which the average orbit does not change turn-by-turn. Similar algorithm is also available to adjust RF frequency.

Closed orbit correction Similarly to trajectory correction, the closed orbit is corrected using the theoretical orbit response matrix (filtered with a maximum number of singular vectors or using Tikhonov regularization).

Beam based alignment Performs a trajectory or orbit scan in a BPM together with changing the strength of a neighbouring magnet. Fits result in a BPM reading corresponding to the centre of the magnet.

Tune working point scan Betatron tune working is scanned and the beam transmission is observed and optimised.

Tune and chromaticity Families of quadrupoles and/or sextupoles are used for adjusting the betatron tunes and/or the chromaticity to the desired values. This correction is possible once a closed orbit is established. Tune correction based on trajectory is under development.

Linear Optics from Closed Orbit (LOCO⁵⁵) for the correction of linear optics and coupling based on the measurement of orbit response matrix data. In particular, the closed-orbit correction based on precise measurements recorded at the BPMs in response to current changes at the correcting magnets (ORMs). The LOCO algorithm is used for the linear optics calibration. This involves adjusting

⁵⁵ J. Safranek, Linear Optics from Closed Orbits (LOCO): An introduction, SLAC-REPRINT-2009-545



the parameters of the lattice model and iteratively fitting the response matrices of the model to the measured data to detect machine errors accurately.

The correction methods mentioned above utilize only the information available (directly observable) in a real machine. Thus, the same methods can be used to commission these machines, the only differences being the interfaces to the control system.

Analytical functions to evaluate the simulation progress may use true values of errors and are well separated from the correction functions.

Usage examples

Petra IV

The commissioning chain of PETRA IV starts with various first and second-turn trajectory corrections. A sample of a trajectory being corrected is shown in Figure 36. Once the two-turn trajectory (including the one-turn closed orbit) has been corrected, the typical transmission of about 20 turns is achieved.

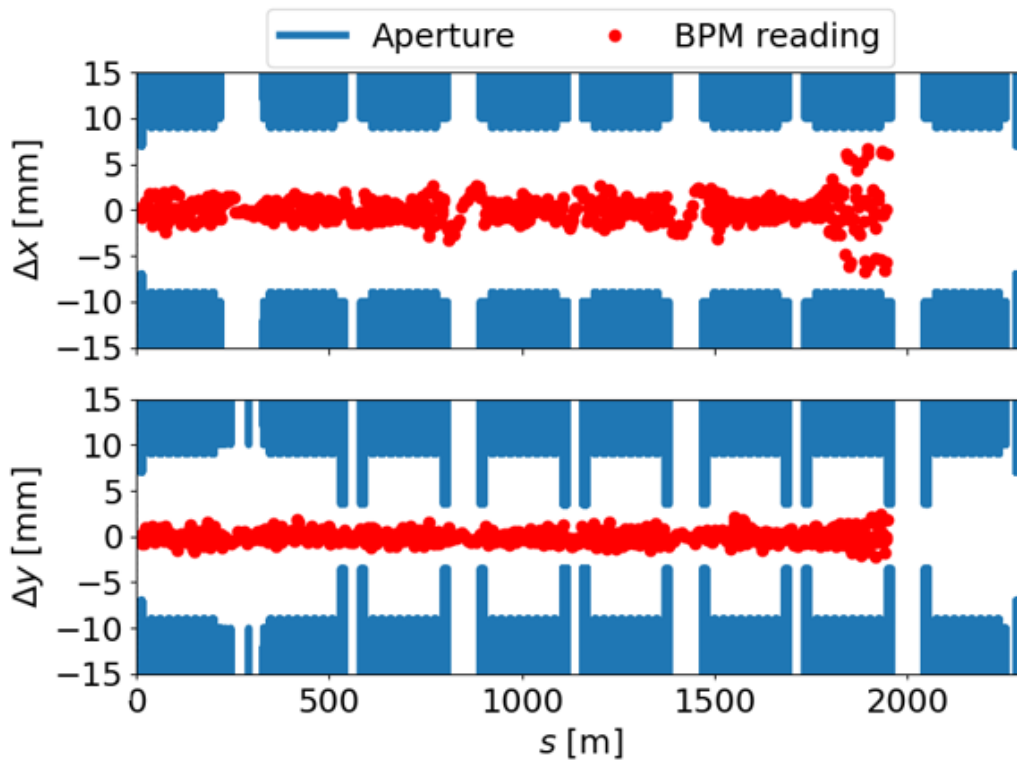


Figure 36: PETRA IV first-turn trajectory correction in progress using pySC

Later, some form of beam-based alignment appears to be necessary, and Figure 37 compares the BPM misalignments with respect to neighboring magnets before and after beam-trajectory-based alignment, i.e. the figure only analyzes the process of commissioning simulation and is therefore not available in actual commissioning.

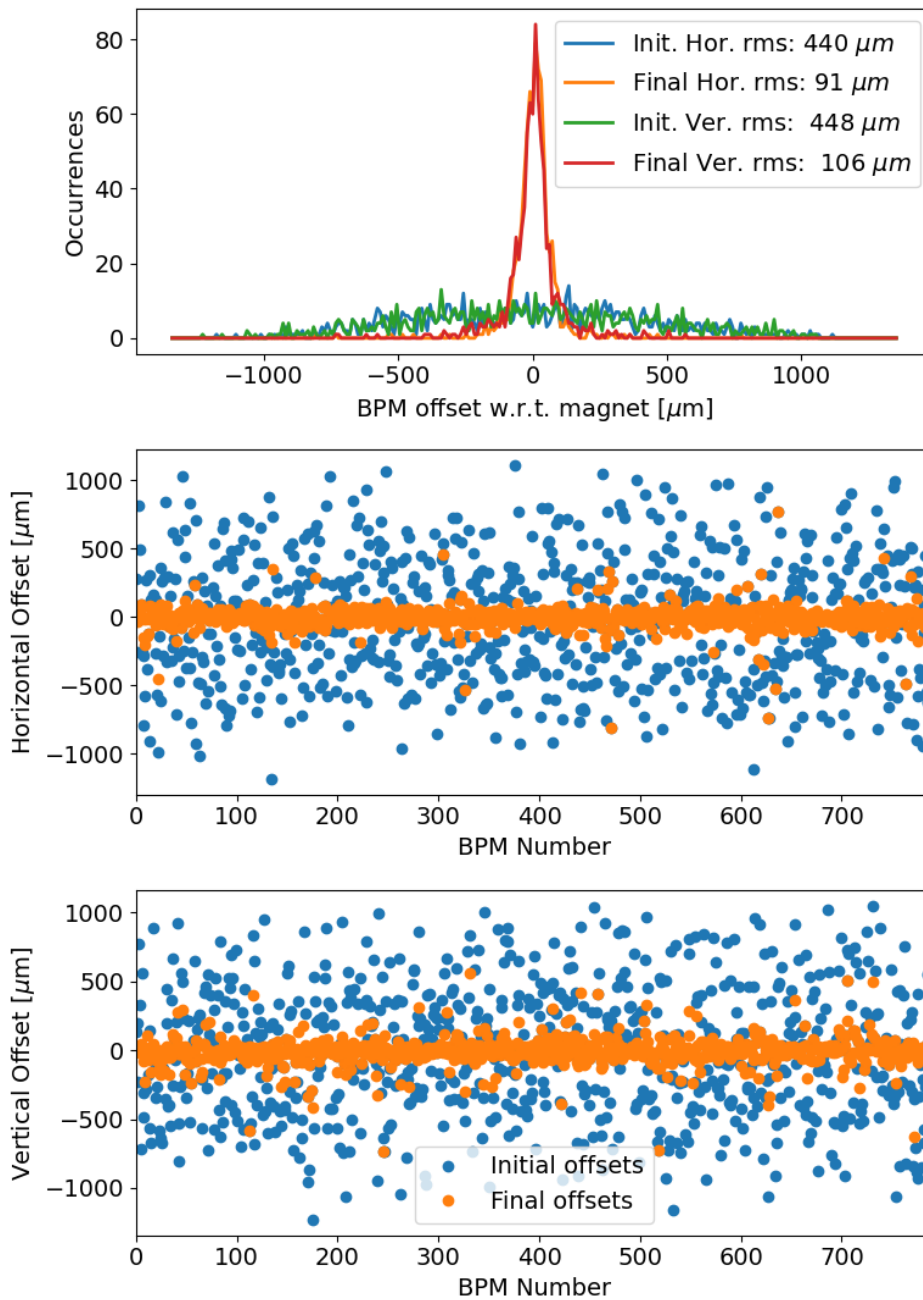


Figure 37: Beam-trajectory-based alignment of PETRA IV BPMs using pySC. The top plot shows distributions of misalignments of BPMs with respect to centers of neighboring magnets: initial (in blue and green) and final (in red and orange). Middle and bottom plots show individual horizontal and vertical misalignments before alignment (in blue) and after alignment (in orange).

With the RF system still off, the typical transmission is limited to less than 100 turns due to energy lost via synchrotron radiation. Therefore, switching on and setting up the RF system (mostly phase and frequency) is vital. A full RF phase scan result is shown in Figure 38. Needless to mention, the result is fully observable, unlike the BBA example.

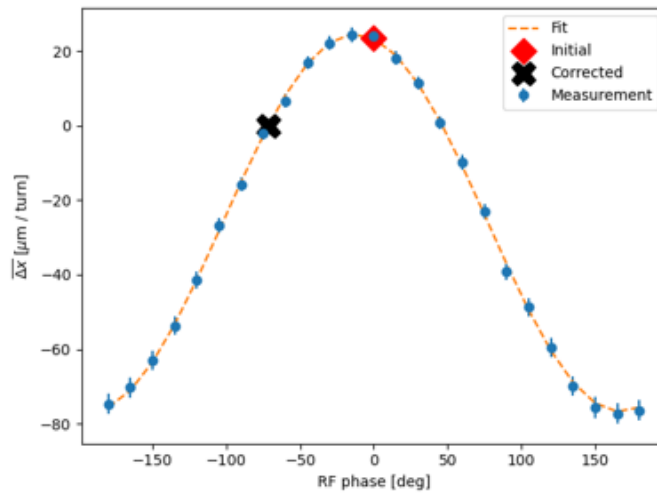


Figure 38: Fitted change of average trajectory turn-by-turn as a function of RF phase. The correction algorithm searches for zero-crossing, where the RF system replenishes the lost beam energy via synchrotron radiation.

Similarly, the RF frequency is corrected, leading to most of the injected beam transmitted through 1000 turns, as shown in Figure 39 and the establishment of a closed orbit.

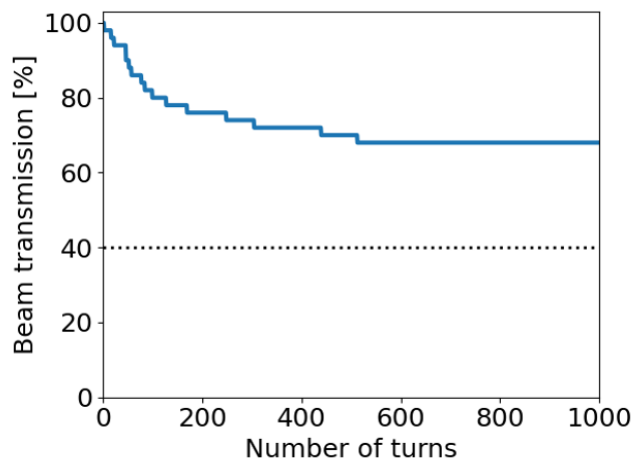


Figure 39: Typical PETRA IV beam transmission after RF phase and frequency correction.

ESRF-EBS

The pySC code is tested for the EBS lattice. Uncertainties are registered and applied in the lattice using the *register** methods and *apply_errors*. The errors used are the alignment of quadrupoles and sextupoles of 60 μm rms in both planes and gradient errors in those magnets, for simplicity. With these errors, there is no single turn possible in EBS.

Figure 40 shows how the trajectory/orbit correction functions can achieve transmission through the first turn and a corrected closed orbit without switching the sextupoles off.



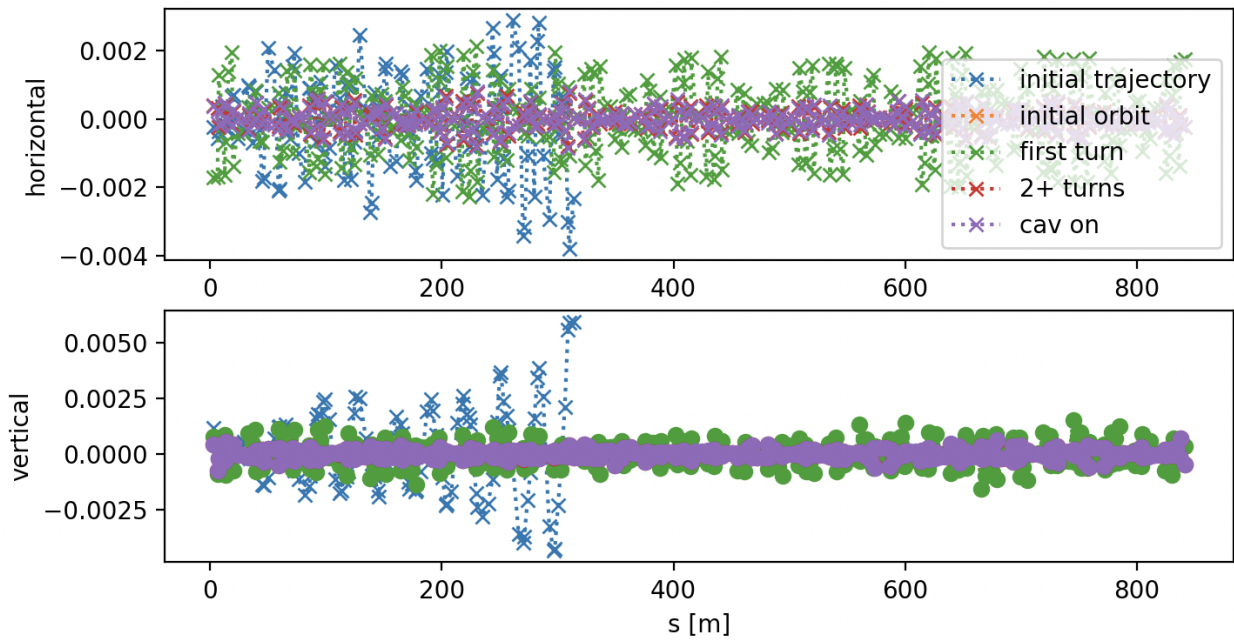


Figure 40: Trajectory and orbit correction for EBS using pySC.

Once closed orbit correction is achieved, pySC is instructed to run tune working point scan to optimize the transmission over the maximum possible number of turns or higher transmission rate. Figure 41 depicts such a step of the correction. This computation is triggered only if no transmission over 200 turns is achieved.

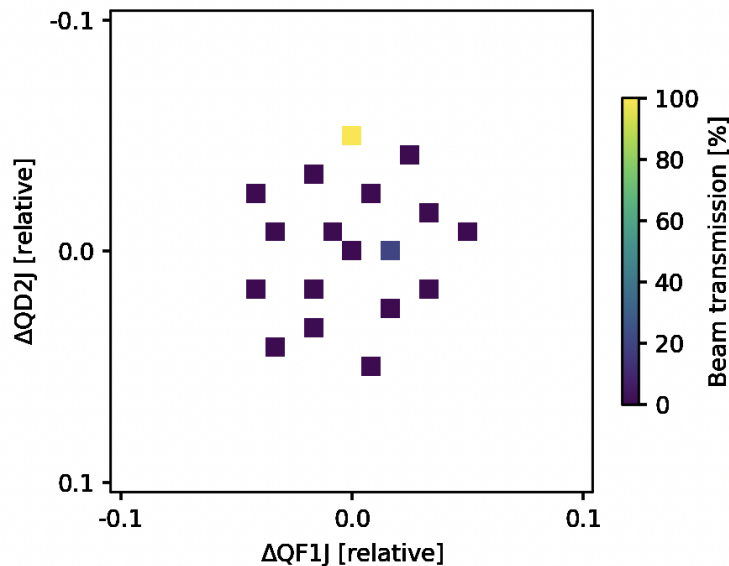


Figure 41: Tune working point scan to increase transmission efficiency.

ALS-U

The ALS-U Storage Ring correction chain⁵⁶ has begun to be ported into pySC. Preliminary steps include the registration of error sources and trajectory correction. For example, Figure 42 shows one lattice cell, including the registered diagnostic devices.

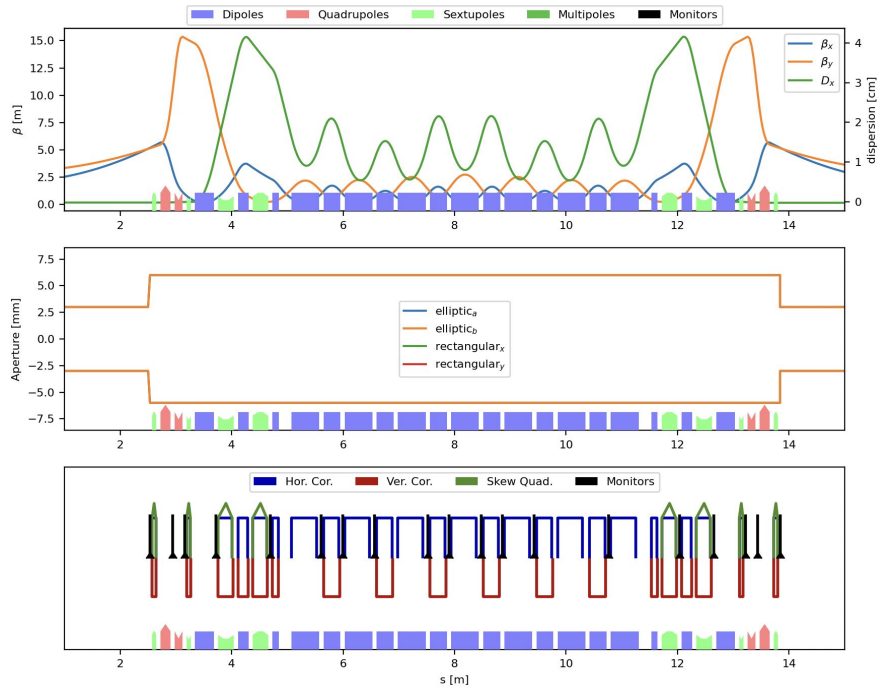


Figure 42: ALS-U Storage Ring cell as registered in pySC.

PySC summary and future work

A new library written in Python and based on standard widely used and well-tested software components, such as NumPy, has been developed and we are approaching its first (alpha) release. At the time of writing, it features more maintainable code measured by CodeClimate, and many automated tests run on every commit.

Some of the correction algorithms have been elaborated utilizing all the available statistical information.

The effort to increase code maintainability, test coverage and performance will continue. Further elaboration of correction methods with modern statistical tools is also planned. This way, the commissioning simulation chain's automation level may increase and the necessary user input decrease.

Future plans for pyAT developments

Due to the many ongoing upgrade programs, there is a growing need in the accelerator community to perform beam commissioning and errors specification simulations. In an effort to make the numerical

⁵⁶ PhysRevAccelBeams.25.110701



tools available and ready to use in an existing well-established environment we have plans to integrate the functionalities needed to perform these simulations in pyAT directly.

In this spirit, several developments are presently ongoing:

- build objects allowing to observe or vary arbitrary accelerator quantities and subsystems as present and available in real accelerator
- define a framework for lattice errors definition and management
- define a framework for lattice corrections

These basic bricks can be applied to accelerator design as well as operation and have to be thought of in such a way that they are flexible enough to be integrated in numerical tools with diverse applications. This would eventually allow us to switch back and forth from the simulation environment to the real accelerator but also from one machine to the other seamlessly and apply the same algorithms with minor adjustments.

Other activities related to the Task 4.1

A total of 5 visits among ESRF and DESY colleagues took place during the EURIZON Task 4.1 activities.

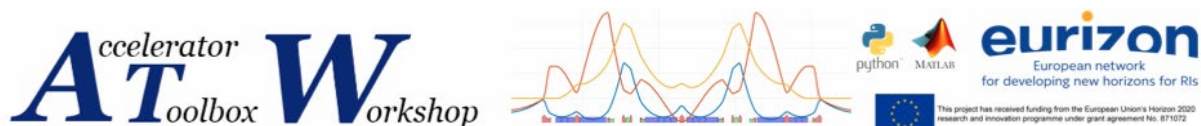
- EBS restart visit in August 2022 with the participation of the members of the project to machine re-commissioning after the summer shut down.
- A visit for machine dedicated time (MDT) on turn by turn data taking.
- A visit for machines dedicated time on Vertical/Emittance and Lifetime optimizations.
- Two visits for machine dedicated time Badger optimization in PETRA III.

All relevant Eurizon Task 4.1 members were invited for participation in remote MDTs.

24 meetings were organized and the relevant information and minutes are available online (<https://indico.esrf.fr/category/2/>).

One main workshop event was prepared to disseminate the results of Eurizon to a larger community. This activity is detailed in the following.

AT workshop on 2-3rd October⁵⁷



The DESY-ESRF collaboration opened the discussion on the Accelerator Toolbox codes, both on Matlab (referred to as AT) and on Python (pyAT) and its applications in the framework of a dedicated workshop. The Accelerator Toolbox workshop was held both remotely and in person on October 2-3 2023 at the ESRF, Grenoble, France. Sixty-eight scientists and developers reunited, presented their applications, modifications and suggestions on the AT/pyAT code for beam dynamics in charged

⁵⁷ <https://indico.esrf.fr/event/93/>



particle accelerators. The workshop program consisted of plenary talks and discussions and included a tunnel visit of the ESRF-EBS storage ring and injectors and a training session on AT and pyAT for willing participants. The program was divided into several sections:

- Status of the Accelerator toolbox codes,
- Beams dynamics in AT and pyAT,
- Measurement and corrections,
- Inspiration and interaction with other codes,
- AT in control room: Middle Layer,
- Future developments.

In preparation of the workshop, a survey was sent to the participants, opening the submission of talks, subjects and speakers. The program was then defined by a Scientific Committee, composed of six AT expert users worldwide.

Results of the survey

The introduction to the workshop presented the development paths of the Accelerator Toolbox, from its origin to its most recent additions (pyAT for example). Development is now mostly conducted by ESRF collaborators, and is in dire need of feedback from its users. Some was provided through the aforementioned survey: eleven different institutes answered, and unanimously supported the hold of the workshop. Out of the 19 respondents, 47% are exclusive users of AT in Matlab, 21% only use pyAT and 32% use both codes. Most users cloned the latest git repository (74%) released version. If the latest pyAT version is used by its users (0.3.0), the AT Matlab version was frozen in many institutes at different stages of development for convenience; these users do not benefit from the latest developments, corrections and additions available in the git version of AT. AT is used for (70%) simulations and modeling (lattice design (42%), injection (24%), commissioning (12%) and feedback (6%)), (25%) operation and control room (through Matlab Middle Layer as well) and (4%) for code development. 65% of the respondents integrate AT in their control systems.

Few people participate in the development of the AT code. Its continuous development provides fast corrections of spotted bugs, latest additions and follows its users' needs. Nonetheless, this approach does not ensure backward compatibility, documentation on the latest changes updated on a weekly basis. This approach remains satisfactory for 33% of the respondents, not for 11% and 56% are undecided. More frequent and stable releases in Matlab and Python could be of interest for 53% of the respondents, the others 47% undecided. This latest point requires more code reviewers and debuggers.

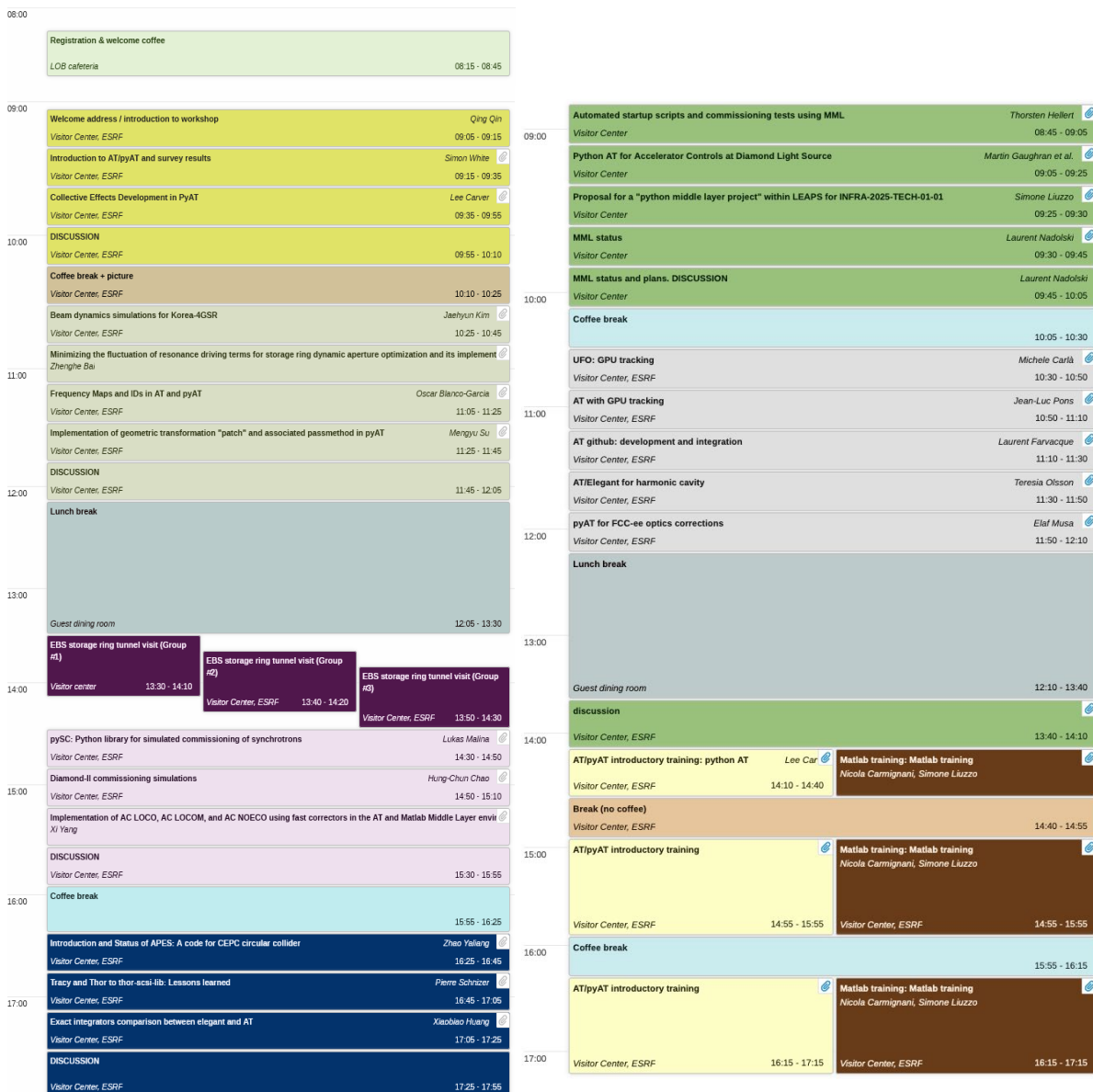
The documentation of AT is satisfactory for 47% of the respondents, not for 6% and 47% think it should be extended or improved. The pyAT documentation is automatically generated using the Sphinx package. This principle could be extended in Matlab, but requires all documentation entries to be translated into a Matlab-compatible documentation program.

The latest additions to pyAT were introduced: main ones include the multi-bunch simulations, which allow parallelisation for collective effects (CE) simulations, and new CE passmethods (WakeFieldPass and BeamMoments).



Main topics discussed:

- recent upgrades of the software and future plans and directions,
- experience of use for simulations: commissioning, DA, Injection efficiency and lifetime, impact of ID gaps on optics, losses & collimation, injection, optics design, optics matching, etc,
- experience of use of AT in control room: MML, Pytac, digital twins, etc,
- use of AT for collective effects studies,
- discussion on code status, maintenance and priority for future developments.



Conclusions

The outcome of the discussions during Milestone meetings M4.1.1, M4.1.2 and M4.1.3 has been the definition of the following specific list of activities:

4. Study the impact of magnetic cross talks among neighboring magnets in the H7BA lattice of EBS and H6BA lattice of PETRA IV.
5. Machine Dedicated Time (MDT) experimental activities at EBS and PETRA III for storage ring optimizations:
 - a. Using available optimizers, among which Extremum Seeker⁵⁸ and Badger⁵⁹+XOpt⁶⁰
 - b. Measurement and analysis of TbT data analysis to determine Storage ring optics
6. Definition of new functions for errors and correction based on pyAT for commissioning simulations of new storage ring projects.

The activities listed above are detailed in the following sections. Point 1 could not be fully investigated for lack of data. Nevertheless, several studies have been performed assessing the effect of cross talks in correctors and quadrupole for PETRA-IV and the effect of longitudinal multipole distributions for EBS. Point 2.a led to successful optimization of lifetime, DA and injection efficiency for both EBS and PETRA-III. The tools developed are now available in the EBS and PETRA-III control rooms for use. Point 2.b activities achieved a first measurement of optics from TbT data for EBS and PETRA-III. The studies were limited by hardware issues (BPM synchronization) and available MDT time and resources. Point 3 resulted in a first version of python commissioning simulations (pySC) package, analytical tools for fast Jacobian computations and a global plot/data storage framework for correction and tuning of lattices with errors.

⁵⁸ A. Scheinker, "Model independent beam tuning", IPAC 2013, TUPWA068

⁵⁹ Zhang, Zhe, and USDOE. Badger: The Ocelot Optimizer Rebirth. Computer software. <https://www.osti.gov/servlets/purl/1874964>. USDOE. 4 Aug. 2021. Web. doi:10.11578/dc.20220706.3.

⁶⁰ R. Roussel, C. Mayes, A. Edelen, A. Bartnik, Xopt: A simplified framework for optimization of accelerator problems using advanced algorithms, *JACoW IPAC2023 (2023) THPL164*, [10.18429/JACoW-IPAC2023-THPL164](https://doi.org/10.18429/JACoW-IPAC2023-THPL164)



Publications

Several publications resulted from EURIZON Task 4.1 activities or were written by the authors on topics closely related to EURIZON Task 4.1.

IPAC 2023

S. Liuzzo *et al.*, “Commissioning simulations tools based on python Accelerator Toolbox”, presented at the IPAC’23, Venice, Italy, May 2023, paper MOPA142, accepted for publication in IOP light peer review.

A. Franchi, S. Liuzzo, and Z. Martí, “Analytic derivative of orbit response matrix and dispersion with thick error sources and thick steerers implemented in python”, presented at the IPAC’23, Venice, Italy, May 2023, paper MOPL069.

B. Veglia *et al.*, “Extremum seeking for accelerator optimisation”, presented at the IPAC’23, Venice, Italy, May 2023, paper MOPA137.

J. Keil, I. Agapov, A. Alov, R. Bartolini and M. Thede,, “Cross-talk between magnets in the H6BA-cell of PETRA IV”, presented at the IPAC’23, Venice, Italy, May 2023, paper WEPM032.

ICALEPCS 2023

S.Liuzzo et al., “Optimisation of the Touschek Lifetime in Synchrotron Light Sources Using Badger”, Cape Town, South Africa, 2023, paper MO3AO01, being published.

L.Malina et al., “Python library for simulated commissioning of storage-ring accelerators”, Cape Town, South Africa, 2023, paper FR2AO05, being published.

